

12-1-2013

Temperature Trends and Urban Heat Island Intensity Mapping of the Las Vegas Valley

Adam Leland Black

University of Nevada, Las Vegas, blacka@unlv.nevada.edu

Follow this and additional works at: <https://digitalscholarship.unlv.edu/thesesdissertations>



Part of the [Climate Commons](#), and the [Remote Sensing Commons](#)

Repository Citation

Black, Adam Leland, "Temperature Trends and Urban Heat Island Intensity Mapping of the Las Vegas Valley" (2013). *UNLV Theses, Dissertations, Professional Papers, and Capstones*. 1975.
<https://digitalscholarship.unlv.edu/thesesdissertations/1975>

This Thesis is protected by copyright and/or related rights. It has been brought to you by Digital Scholarship@UNLV with permission from the rights-holder(s). You are free to use this Thesis in any way that is permitted by the copyright and related rights legislation that applies to your use. For other uses you need to obtain permission from the rights-holder(s) directly, unless additional rights are indicated by a Creative Commons license in the record and/or on the work itself.

This Thesis has been accepted for inclusion in UNLV Theses, Dissertations, Professional Papers, and Capstones by an authorized administrator of Digital Scholarship@UNLV. For more information, please contact digitalscholarship@unlv.edu.

TEMPERATURE TRENDS AND URBAN HEAT ISLAND INTENSITY MAPPING
OF THE LAS VEGAS VALLEY AREA

By

Adam Leland Black

Bachelor of Science in Civil Engineering

University of Nevada, Las Vegas

2009

A thesis submitted in partial fulfillment of the requirements for the
Master of Science in Engineering

Department of Civil and Environmental Engineering and Construction

Howard R. Hughes College of Engineering

The Graduate College

University of Nevada, Las Vegas

December 2013



THE GRADUATE COLLEGE

We recommend the thesis prepared under our supervision by

Adam Black

entitled

Temperature Trends and Urban Heat Island Intensity Mapping of the Las Vegas Valley

is approved in partial fulfillment of the requirements for the degree of

Master of Science in Engineering -- Civil and Environmental Engineering

Department of Civil and Environmental Engineering and Construction

Haroon Stephen, Ph.D., Committee Chair

Jacimaria Batista, Ph.D., Committee Member

Sajjad Ahmad, Ph.D., Committee Member

Daniel Thompson, Ph.D., Graduate College Representative

Kathryn Hausbeck Korgan, Ph.D., Interim Dean of the Graduate College

December 2013

ABSTRACT

Modified urban climate regions that are warmer than rural areas at night are referred to as Urban Heat Islands or UHI. Islands of warmer air over a city can be 12 degrees Celsius greater than the surrounding cooler air. The exponential growth in Las Vegas for the last two decades provides an opportunity to detect gradual temperature changes influenced by an increasing presence of urban materials. This thesis compares ground based thermometric observations and satellite based remote sensing temperature observations to identify temperature trends and UHI areas caused by urban development.

Analysis of temperature trends between 2000 and 2010 at ground weather stations has revealed a general cooling trend in the Las Vegas region. Results show that urban development accompanied by increased vegetation has a cooling effect in arid climates. Analysis of long term temperature trends at McCarran and Nellis weather stations show 2.4 K and 1.2 K rise in temperature over the last 60 years.

The ground weather station temperature data is related to the land surface temperature images from the Landsat Thematic Mapper to estimate and evaluate urban heat island intensity for Las Vegas. Results show that spatial and temporal trends of temperature are related to the gradual change in urban landcover. UHI are mainly observed at the airport and in the industrial areas. This research provides useful insight into the temporal behavior of the Las Vegas area.

ACKNOWLEDGMENTS

I would like to thank the Nevada Division of Forestry for their support and contributions that made this research possible. I also express my appreciation towards Dr. Craig Palmer, Dr. Sajjad Ahmad, Dr. Jacimaria Batista, and Dr. Daniel Thompson for their participation and input. My gratitude will always be given to Dr. Haroon Stephen and my family, Heather, Abigail, and Kaylee. Their patience and committed time with my studies helped me to reach this important accomplishment and has bettered my life.

TABLE OF CONTENTS

ABSTRACT.....	iii
ACKNOWLEDGMENTS	iv
TABLE OF CONTENTS.....	v
LIST OF TABLES	vii
LIST OF FIGURES	viii
CHAPTER 1: Introduction	1
1.1 Background	1
1.2 Research Motivation	4
1.3 Research Objectives	5
1.4 Thesis Outline	5
CHAPTER 2: Literature Review	6
2.1 Urban Heat Island Effect.....	6
2.2 Urban Layers	7
2.2.1 Surface Layer	8
2.2.2 Canopy Layer.....	10
2.2.3 Urban Boundary Layer	12
2.3 Urban Energy Balance Equation.....	13
2.4 Data Sources.....	16
2.4.1 Weather Stations	16
2.4.2 Remote Sensing	18
2.5 Las Vegas Valley	19
CHAPTER 3: Data and Methods.....	28
3.1 Research Approach	28
3.2 Data	31
3.2.1 Meteorological Temperature Measurements	31
3.2.2 Remote Sensed Images	36
3.2.3 Zoning and Planned Land Use Boundaries.....	38
3.2.4 Southern Nevada Water Authority 2006 Canopy Data.....	40
3.3 Temperature Trend Analysis at Weather Station Locations	41
3.3.1 Low-pass Filter Approach.....	42
3.3.2 Sinusoidal Model Approach	44
3.3.3 Temperature Anomaly Trend Approach.....	47

3.4	Spatial Behavior of Temperature Trends and Urban Heat Island Intensity	49
3.4.1	Urban Heat Island Intensity Image	50
3.5	Summary	52
CHAPTER 4:	Temperature Trend Analysis at Weather Station Locations.....	53
4.1	Low-pass Filter Analysis.....	53
4.2	Sinusoidal and MDM modeling analysis	54
4.3	Trend Analysis of Temperature.....	55
4.4	Trends Relation to NDVI Change	60
4.5	Long term Temperature Trends.....	63
4.6	Summary	64
CHAPTER 5:	Spatial Behavior of Temperature Trends and Urban Heat Island Intensity	67
5.1	UHII from Regression Model of Wunderground and Landsat Temperature	67
5.2	Las Vegas Valley Integrated Zone Map.....	77
5.3	Temperature Trend Analysis of Landsat Thematic Mapper Temperature Data	78
5.4	Summary	79
CHAPTER 6:	Summary, Conclusions, and Recommendations	81
6.1	Conclusions	81
6.2	Limitations	84
6.3	Recommendations for Future UHI Analysis.....	85
APPENDIX A:	Merged PLU Table of Las Vegas.....	87
APPENDIX B:	Definition of Local Climate Zones (Stewart and Oke, 2012)	88
APPENDIX C:	Parameters of the Midnight and Noon Air Temperature Models.....	89
Midnight Air Temperature Model Regression and Correlation Parameters		89
Noon Air Temperature Model Regression and Correlation Parameters		90
REFERENCES	91
VITA	98

LIST OF TABLES

Table 1: Weather Underground Station List.....	32
Table 2: Referenced Figures and Shapefiles Used to Create a Unified Land Use Map of Las Vegas.....	39
Table 3: Low-pass Filter Temperature Trends.....	53
Table 4: List of Ground Stations Showing Period of Temperature Data and Landuse ...	54
Table 5: Model Parameters Using Sinusoidal and Residual Methods for All Ground Stations.....	57
Table 6: Mean Change in Temperature by Zone Type	78

LIST OF FIGURES

Figure 1: Urban layer locations (Reducing Urban Heat Islands, 2008).....	8
Figure 2: Las Vegas disposal boundary and city locations.....	21
Figure 3: Las Vegas population growth between 1990-2011.....	22
Figure 4: Comparison of 1990 vs. 2010 aerial view of Las Vegas.....	22
Figure 5: Research method flowchart.....	30
Figure 6: Weather station locations in Las Vegas valley.....	33
Figure 7: Sample plot of temperature data vs. time for weather station 13.....	34
Figure 8: Diurnal temperature variation for station 13 on Aug. 27, 2010.....	35
Figure 9: Unified landuse map of Las Vegas.....	41
Figure 10: Diurnal comparison of weather stations experiencing different strengths of UHI.....	51
Figure 11: Plot showing time series of daily average temperature at Palomino Estates ground station with sinusoidal model fit and trend line.....	55
Figure 12: (top) Multiyear Daily Mean curve computed from all annual cycles and (bottom) Time series of the residual temperature.....	56
Figure 13: Las Vegas urban change between (left) 2000 and (right) 2010 as viewed by Landsat 5 Thematic Mapper.....	59
Figure 14: Spatial distribution of NDVI in the (left) 2000 and (right) 2010.....	61
Figure 15: Spatial distribution of NDVI change between 2000 and 2010.....	62
Figure 16: Plot of NDVI change vs. temperature change at all the ground stations between 2000 and 2010.....	62
Figure 17: Long-term temperature trend using Multianual Daily Mean approach at (top) McCarran Airport and (bottom) Nellis Air Force Base.....	63
Figure 18: Long-term temperature trend excluding last decade using Multianual Daily Mean approach at (top) McCarran Airport and (bottom) Nellis Air Force Base.....	64
Figure 19: Graph showing a multi-year time series of air temperature observations and LST at station 11.....	68
Figure 20: Graph showing typical diurnal variation of air temperature observations with LST from Landsat thermal imagery at 10AM at station 11.....	68
Figure 21: Graph showing relationships between average LST and (a) midnight air temperature and (b) noon air temperature at station 11.....	69
Figure 22: Images of linear model parameters for midnight [(a) and (b)], and noon [(c) and (d)].....	70
Figure 23: Images of estimated midnight (left) and noon (right) air temperature for June 27, 2011.....	71
Figure 24: Urban Heat Island Intensity map of Las Vegas on June 27, 2011 (top), land surface temperature at 10:00 AM (bottom left), and Landsat 5 true color composite image (bottom right).....	72
Figure 25: UHII map of Las Vegas on June 27, 2011 overlaid with SNWA 2006 tree canopy data.....	73
Figure 26: (Right) Urban Heat Island Intensity map of Las Vegas (Left) Landsat 5 true color composite image.....	76

Figure 27: (Right) Urban Heat Island Intensity map of Las Vegas (Left) Landsat 5 true color composite image. 77

Figure 28: Spatial map of temperature trend estimated from Landsat TM 1990-2010 data. 79

CHAPTER 1: Introduction

It has become increasingly evident that large developments influence the climate within the immediate region (Taha, 1997). There are concerns that rising temperatures over developed areas could have negative impact on the local environment and increase living discomfort within city boundaries. An urbanized region exhibiting higher atmospheric temperatures than nearby rural lands untouched by anthropomorphic influences is called an Urban Heat Island (UHI). Research indicates that UHI exists year round and the intensity is the greatest during the evenings. It is important to identify areas experiencing abnormal temperature changes to better understand the relationship between surface cover and near surface air temperatures.

Temperature trends in Las Vegas have received minor attention, yet the area has experienced heavy urban expansion between 1980 and 2010. This area provides an opportunity to observe the effects of city growth on the temperature in an arid environment. This thesis analyzes atmospheric temperature observations from several meteorological stations and land surface temperature from satellite remote sensors to establish historical temperature trends, identify UHI locations, and UHI intensities in the Las Vegas valley. Trends are compared to land use and land cover (LULC) to evaluate the relationship between temperature behavior and urban growth in Las Vegas, Nevada.

1.1 Background

UHI refers to the raised nighttime air temperature of developed areas when compared with nearby rural surroundings. The replacement of the natural landscape through city expansion can increase the nighttime atmospheric temperature by at least 2

to 3 Kelvin (K). The increase of evening temperature is attributed to surface heat transfer properties, increased impervious surface area, change in surface geometry, and anthropomorphic activities.

The main contributor to UHI is the properties affecting heat retention and transfer from urban surfaces to the cooling atmosphere in the evening. Urban material properties cause surfaces exposed to sunlight to attain high land surface temperatures (LST). Urban surfaces absorb and retain solar radiation during clear, sunny days. Irradiated urban surfaces then transfer the stored heat energy to the near surface air (boundary layers) by radiation and conduction throughout the evening.

Moist environments comprised of dense vegetated areas primarily experience occurrence of latent heat transfer between the ground surface and the atmosphere. Latent heat transfer is the exchange of energy within a system without changing the temperature. Water located in vegetation, irrigation, and ground water at the surface absorbs heat energy from the ground. The absorbed energy causes the water to evaporate in an isothermal process and dissipate into the atmosphere. Thus, vegetation can regulate the temperature and reduce the intensity of UHI effect.

Replacement of natural vegetation with impervious surfaces reduces the moisture content of the environment. With low moisture available for latent heat transfer, the majority of the surface energy is dissipated as sensible heat. Sensible heat transfer induces a change in temperature of the involved media. Without moisture, surfaces directly transfer heat energy to the atmosphere by radiation. This elevates the temperature of the atmosphere as the surface cools.

Geometry of urban structures plays a key role through increasing the surface area and changing the surface roughness. The large surface area in the street corridors forms urban canyons that is not fully open to the atmosphere and thus is prevented from radiating into the atmosphere. Increased surface roughness affects the local aerodynamics and may reduce air movement impacting the convective cooling.

Finally, anthropomorphic activities in populated areas encourage elevated temperatures, although it has been shown that the effects can be very slight in the urban center or even negligible in the residential suburban regions (Taha, 1997). Air conditioning units pump heat to the atmosphere to cool enclosed environments. Moreover, heavy traffic in high populated areas also generates greenhouse gases.

There are concerns that UHI formation can impact several urban living conditions already linked to temperatures. Air temperatures can cause thermal discomfort and affect energy consumption, air quality, and population health. Increased nighttime temperatures would prolong thermal discomfort that is experienced during the daytime and encourage increased energy consumption through extended use of air conditioning units. Increased generation of electricity to power cities contributes to greenhouse gases and other air pollutants that affect city air quality. Sustained high temperatures also elevate the creation of ground-level ozone, which typically occurs during hot weather (Lo, 2003; Zha 2012).

Extended exposure to elevated temperatures during warmer months would also increase the likelihood of heat related illnesses and deaths. These include population susceptibility to dehydration, heat exhaustion, heat stroke, respiratory difficulties and

several other health concerns, which greatly increase for temperatures exceeding 300 K (Frumkin, 2002).

The determination of heat island areas by comparing meteorological weather data and remotely sensed satellite images can identify areas that need attention. Management of UHI problem areas in a city could help reduce the negative effects of urban development and improve living conditions by improving urban infrastructure and practices.

1.2 Research Motivation

The Las Vegas valley is a densely populated urban center consisting of the cities of Las Vegas, North Las Vegas, and Henderson. The city is located within the Mojave Desert near Lake Mead in southern Clark County, Nevada. Temperatures in this region can range from 280 K in the winter to over 315 K during the summer. Las Vegas is currently the largest populated region of the state. The city has maintained a 5.6% annual population increase for several years. The number of residents has more than doubled between 1990 and 2010 from around 900,000 to over 2 million people. This substantial increase in population in Las Vegas has encouraged intense construction activities during this period which has led to a rapid expansion of the urban area in the Las Vegas valley. The fast paced urban expansion in this region provides an opportunity to analyze UHI growth in an arid environment. Moreover, investigation into improving UHI mapping methods can be beneficial in determining what development factors contribute to UHI formation.

1.3 Research Objectives

This thesis analyzes UHI in Las Vegas by studying spatial and temporal trends of temperature observations. Ground based thermometric observations and satellite based remote sensing temperature observations are used to conduct research. This research addresses the following questions.

1. What are the temperature trends in the Las Vegas valley caused by urban development?
2. What is the relationship between land surface temperature and air temperature in the Las Vegas area? How can this relationship be used to identify UHI locations?
3. What is the relationship of land use and land cover with UHI development in an arid environment?

1.4 Thesis Outline

This thesis is comprised of six chapters. Chapter one introduces the topic of UHI and states the objective of the research performed. Chapter 2 is a literature review which defines UHI, describes current modeling methods and applications, and research performed for the Las Vegas area or similar climate regions. The third chapter describes the data and research methodology used for analysis. Chapter 4 presents temperature trend results obtained from point weather station observations. Chapter 5 presents spatial analysis results in the form of UHI intensity images of Las Vegas area by correlating point weather station temperature observations with remote sensed LST images. Chapter 6 provides summary, conclusions and future research recommendations.

CHAPTER 2: Literature Review

This chapter provides a review of research articles on the subject of UHI, and explores current research related to urban effects on local climates. This includes a description of the Weather Underground services, and the Landsat program. The chapter concludes with an historical account and description of the urban growth in the Las Vegas area. Previous temperature trend and UHI analyses of the Las Vegas valley are also described to establish a research baseline.

2.1 Urban Heat Island Effect

Urban regions exhibit differing climate characteristics and weather patterns than adjacent rural areas (Taha, 1997). Development of rural land drastically changes the surface composition and characteristics leading to inadvertent climate modifications in urban areas (Oke, 1978, Lo 1997). One of the regional climate characteristics that is altered by developed land are the heating and cooling rates of the ground and atmospheric temperatures. Changes in the surface properties produce regions that are warmer than the surrounding natural surface. A region of warm air or surface enclosed by cooler air or surface is called a heat island.

Heat islands effect was first noted by Luke Howard in 1818 where he observed that the temperature records at the Royal Society in London were always greater than temperature readings at three rural weather stations outside the city of London (Howard, 2011). Continued investigation into this urban phenomenon in cities around the world has shown that Luke Howard's observations were not an isolated incident.

The effect of urban development on air temperatures is a regionally confined phenomenon (Reducing urban heat islands 2008), whereas a global climate change is an environmental modification experienced worldwide such as the greenhouse gas effect causing global warming. Urban regions of high temperatures are limited to a local scale that rapidly decreases with distance from the source. The footprint is limited by the heat energy available to sustain an elevated temperature for large regions. There should be some point beyond which any further addition of urban fabric becomes climatically less significant. Oke was able to show this by plotting city temperatures versus the population density of the area. His findings show that heat islands have an approximate logarithmic relation with population (Oke, 1973). That is, an increase in urban density has more effect on regional temperatures in a small town than a large city.

Researchers have developed and applied the concept of urban energy balance to their analysis to better understand how heat energy flows within a city environment. The basis of this concept is to define a control volume containing the urban environment being analyzed and balances the total energy leaving and entering the system. Oke defines three urban layers to establish the boundaries of the control volume (Oke, 1978; Oke, 1988).

2.2 Urban Layers

Heat island analysis in an urban environment is separated into three different layers. These urban layers are the surface layer, the canopy layer, and the urban boundary layer. Layer boundaries and location are presented in Figure 1. The surface layer consists of the ground surfaces that are in direct contact with atmosphere. The

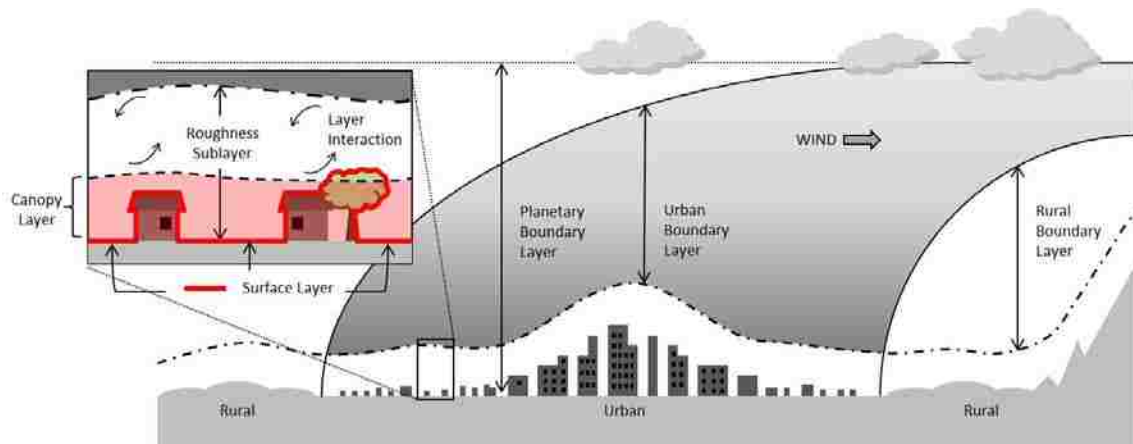


Figure 1: Urban layer locations (Reducing Urban Heat Islands, 2008).

canopy layer is the portion of atmosphere between the surface layer and the rooftops of urban dwellings. The urban boundary layer is the atmosphere region above an urban development that is influenced by heat transfer from the canopy layer. The characteristics and mechanics of heat islands differ between these three layers (Arnfield, 2003). Yet, the behavior of the heat islands is dependent on the interaction between the layers.

2.2.1 Surface Layer

The surface layer is the lowest layer of the urban environment where the ground surface is in contact with the Earth's atmosphere. The majority of net solar radiation absorption occurs at the surface layer making the surface the warmest of the soil and atmosphere system (Oke, 1978). Ground surfaces are warmed by solar radiance during the day and release as latent and sensible heat energy to the atmosphere during the evening. Surface thermal properties are a key component to surface energy balance and influence the air temperatures directly above the surface (Xian, 2006).

The most common method to analyze surface temperatures is with remote sensing techniques (Weng, 2004; Buyantuyev, 2010). A surface that radiates thermal energy also

emits spectral radiance in the thermal infrared region of the light spectrum between 3 μm and 20 μm (*Landsat 7*, 2008). The strength of the spectral radiance detected in the thermal infrared region of the spectrum can be used to approximate the surface temperature by applying Planck's Law. Satellite remote sensing provides a straightforward and consistent way to determine thermal difference between urban and rural surfaces (Xian, 2006). Remote sensing devices can only determine spectral intensity from visible surfaces, i.e., the temperature cannot be determined for surfaces perpendicular to the field of vision or obstructed by clouds.

A warm surface area contained within a cooler surface region is called a surface urban heat island. Surface heat islands are present at all times of the day and are strongest near mid-day during the summer (*Reducing urban heat islands*, 2008; Buyantuyev, 2010). High surface temperatures in urban areas are attributed to increased impervious surface cover area. Urban centers typically have higher concentrations of dry impervious surfaces (Xian, 2006). Impervious surfaces in urban areas usually have low albedo. US cities have an average surface albedo between 0.15 and 0.2 (Taha, 1997) meaning that 80% to 95% of solar irradiance is absorbed by the surface. Using high albedo materials reduces solar radiation absorbed and keeps surfaces cooler (Taha, 1997).

Impervious surfaces prevent ground infiltration of water runoff which lowers the soil moisture content of the region. This greatly reduces the moisture available to dissipate heat through latent heat transfer process of evaporation (Weng, 2004). These urban surface characteristics can cause surface temperatures that exceed near surface air temperatures by as much as 50 degrees Celsius (*Reducing urban heat islands*, 2008). Surface temperature difference between urban and rural regions is 10 to 15 degrees

Celsius during the day and 5 to 10 degrees Celsius at night (*Reducing urban heat islands*, 2008).

Surface urban heat islands play an important role in the temperature characteristics of the urban layer directly above the surface. High urban surface temperatures become the main radiant heat source of air within the canopy layer after sunset. With the majority of the heat energy transferred from urban surfaces to the air as sensible heat instead of latent heat, the nighttime temperatures increase.

2.2.2 Canopy Layer

The canopy layer is defined as the layer of air between the ground to just below the tree and building rooftops (*Reducing urban heat islands*, 2008). The majority of heat energy is transferred through the urban canopy layer. During the day, solar irradiance passes through the atmosphere to heat the surface layer. After the sun sets, the primary energy transfer is the heat radiation from the irradiated surfaces to the canopy layer.

The most common method of monitoring air temperatures within the canopy layer are with thermometers at meteorological station locations. Observations at a weather station provide historical temperature data at a point. Another method used in analyzing canopy layer temperature behavior is performing a transit with a thermometer in a mobile vehicle to create an approximate geographical temperature profile of a region.

Modified urban climate regions that are warmer than rural areas at night are typically referred to as Urban Heat Islands or UHI (Voogt, 2003). Canopy layer temperatures in dense urban areas average a 2 degree Celsius increase from rural temperatures (Taha, 1997; *Reducing urban heat islands*, 2008). In ideal UHI conditions,

which are clear calm nights during the fall and winter months, this difference can reach 12 degrees (*Reducing urban heat islands*, 2008).

UHI in the canopy layer is observable mainly at night and is strongest in the winter. Comparison of canopy layer temperatures between rural and urban areas shows similar trends in the late morning and throughout the day. In the evening the temperature differences between the two regions become pronounced as the rural canopy layer cools at a quicker rate than the urban canopy layer (*Reducing urban heat islands*, 2008). Maximum UHI typically occurs between 9:00 pm and 11:00 pm (Oke, 1973).

UHI effect is influenced by albedo, evapotranspiration, and anthropogenic heat sources (Taha, 1997). Urban areas have higher solar radiation absorption and a greater thermal conductivity and capacity for releasing heat stored during the day at night (Xian, 2006). Impervious urban surfaces reduce ground water infiltration of irrigation water and vegetation area that reduces evapotranspiration. This decreases the occurrence of latent heat transfer. Anthropogenic sources give of large amounts of heat energy to the atmosphere, although the effect is only noticeable in city centers of densely populated areas (Taha, 1997).

There are factors that limit UHI development. When a city attains a large heat island the urban/rural temperature gradient often becomes sufficient to induce a convergent thermal breeze circulation. This airflow will prevent complete stagnation from occurring, and provides a built-in limit to further heat island growth (Oke, 1973). Also, urban heat sinks develop where urban surfaces replace dry, bare, and low-density native soils (Xian, 2006). The original ground cover closely matches the properties of

urban materials. Typical landscaping practices also increase the vegetation cover and soil moisture. In this situation the canopy climate can experiences a drop in average evening temperatures.

2.2.3 Urban Boundary Layer

The urban boundary layer extends from the city rooftops to point where the urban landscape no longer influences the atmosphere. The effects of the canopy layer upon the urban boundary layer are considered not to extend further than one mile from the surface (*Reducing urban heat islands*, 2008).

Temperatures in the urban boundary layer can be measured using three different methods. Thermometers attached to a fixed tower can measure temperatures at single location. Continuous thermometer readings from an airplane transvers over a city will produce a two dimensional profile of the layer temperature. The urban boundary layer temperature can also be determined remotely with sonic detection and ranging (SODAR) technology from weather balloons.

Air temperatures in the urban boundary have a distinct behavior. Typically, during the day the temperature is warmest nearest the surface and decreases as the elevation increases. In the evening, the urban boundary layer temperatures experiences an inversion in the temperature profile in that the temperature is coolest at the surface and increases as elevation increases (Oke, 1978). This means that the greatest temperature change occurs at the surface and becomes more stable at higher elevations. Warmer air rises from the urban canopy layer increasing evening temperatures in the upper

atmosphere. The energy transferred to the boundary layer is evenly distributed throughout the layer changing the temperature at a meso-scale (Arnfield, 2003).

Urban surface characteristics and changes in temperature within the boundary layer influence weather patterns in the region. Such as lower solar radiation due to urban canyons, more clouds because of increased pollution particles in the upper atmosphere, increased rain and snowfall occurrence because of the increased cloud activity (Taha, 1997).

UHI are strongest on clear calm days. Clouds block solar radiation reducing surface temperatures during the day and winds increase atmosphere mixing blurring the boundary between rural and urban temps (*Reducing urban heat islands*, 2008). Diffusion of UHI less noticeable and indirectly experienced makes the layer less of a research focus.

2.3 Urban Energy Balance Equation

In order to understand the urban heat island effect, it is important to understand the thermal process in the natural environment. All thermal processes are primarily energized by the solar energy and regulated by the natural environment. In the natural environment, the typical constituents of the landscape are rock, soil, water, and vegetation. These constituents respond to solar energy reflection/scattering, transmission, absorption, emission, and metamorphosis. These processes are explained as follows:

Reflection/Scattering is the process where incident energy is reflected back due to the surface reflectivity characteristics and returns into the atmosphere contributing to Earth's albedo.

Transmission is passing-through of the incident energy through the intervening medium where it undergoes volume absorption and scattering. The energy may reach the next layer and undergo another round of absorption/reflection.

Absorption is the process where incident solar energy is absorbed and becomes part of the internal energy of the medium. This is governed by the absorptivity characteristics of the material.

Emission/Re-radiation is the energy emitted back into the atmosphere. In thermal equilibrium, absorption is equal to emission. If absorption is greater than emission, the body's temperature increases and *vice versa*. This is governed by the emissivity characteristic of the material.

Metamorphosis is conversion of incident energy into chemical energy (photosynthesis), mechanical energy (weathering), or electric energy (photoelectric effect).

The net thermal effect of these processes is heating and cooling cycle of the material which is synchronous with the diurnal behavior of solar energy. When the natural terrain is converted into urban terrain, the processes remain the same but the intensity and rates are changed. For example, due to the new materials introduced in the area (concrete, asphalt), the emissive, absorptive, and reflective characteristics change leading to following effects:

1. shift of the thermal equilibrium.
2. energy retention due to high specific heat materials

3. energy entrapment in urban canyons between large buildings
4. overheating or overcooling, and
5. shifts in the diurnal cycle.

These effects lead to creation of urban heat islands or urban cool islands. UHI are the neighborhoods where the area doesn't cool down at night due to blockage at night of the escape routes of the heat energy that was absorbed during the day. Urban cool islands are the areas where the energy intake routes are blocked during the day and it doesn't receive sufficient energy during the day. Either way the thermal equilibrium is shifted to a new balance point.

The urban heat equation is given as

$$Q^* = Q_H + Q_E + Q_G + \Delta Q_S \quad (1)$$

where Q^* is the net all-wave radiation flux density, Q_H is the turbulent sensible heat flux density, Q_E is the turbulent latent heat flux density, Q_G is the sub-surface heat flux density, and ΔQ_S is the change in energy storage to balance the equation (Oke, 1978; Oke, 1988; Arnfield, 2003). Flux densities are measured in Watts per square meter.

Various surface types have different flux density rates. As energy enters or leaves a substance, the temperature changes within the media accordingly. The average energy required to change the temperature of a volume by a degree Kelvin is referred to as the specific heat of the material. Soil is composed of several different kinds of minerals. The specific heat of soil can range between 0.16 and 0.27 cal/g·°C (0.67 and 1.13 kJ/kg·K) (Bowers, 1962). The specific heat of typical building materials such as brick,

concrete, and softwoods range between 0.8 and 1.4 kJ/kg·K (Moran, 2010). Comparison of the two specific heat ranges suggests that more energy is stored within urban surfaces than rural soil surfaces at equivalent temperatures.

2.4 Data Sources

Temperature trends of Las Vegas are studied using data from two sources including ground based and satellite based measurements. First, the thermometric temperature is used from ground based weather stations and second, land surface temperature is derived from thermal infrared Landsat imagery. Landsat derived NDVI data is also used.

2.4.1 Weather Stations

Temperature trends of an area can be modeled from observed weather phenomenon. Thermometers at ground based weather stations measure the air temperature at a geographic point over time. Stations collect high temporal resolution data, but only at one location. Meteorological stations typically detect several weather patterns such as air velocity, turbulence fluctuations, humidity, precipitation and temperature. Weather patterns can be compared to evaluate links of environmental conditions with UHI effect (Arnfield, 2003). Several, evenly distributed stations would need to be used to interpolate an accurate thermal map of a given region.

Air temperature models created from observed weather data can assist in detecting actual occurrences of developing UHI. Ground based weather stations is one of the main resources in gathering temperature field measurements. Weather stations have high upkeep expenses and need to be maintained for years to gather the prerequisite data for trend analysis, but the recorded temperature observations depict actual UHI formations

since the data originates from actual historical events. Weather data used in this analysis originates from an Internet website called the Weather Underground. Several notable studies have used data collected by the Weather Underground in the past (Emmanuel, 2012; Geller 2007).

Weather Underground began as an Internet program to display worldwide real-time weather data developed by University of Michigan faculty and students in 1991. The Internet weather program was redesigned in 1993 to bring weather information into K-12 classrooms. The program was named Weather Underground after a 1960's University of Michigan radical group. In the fall of 1995, the official Weather Underground website was established providing weather forecasts, current weather conditions, and hourly historical data for 550 US cities.

Currently, Weather Underground has the largest personal weather station (PWS) network of approximately 36,000 stations with almost 23,000 located in the US. Strict quality controls are applied to these meteorological stations and observations are recorded approximately every 15 minutes. The website also references weather information from weather stations with the Airport Automated Surface Observation Systems and the Meteorological Assimilation Data Ingest System which are managed by the Federal Aviation Administration, and the National Oceanic and Atmospheric Administration, respectively. Weather conditions for these stations are reported on an hourly basis.

Weather Underground provides Comma Separated Values (CSV) webpages for each PSW day of historical weather observations including temperature, pressure

humidity, and local time of occurrence. Online station location and data links are removed if a weather station is decommissioned, but the data remains accessible using a non-searchable web link.

2.4.2 Remote Sensing

Remote sensing has been used to identify land surface temperatures, vegetation cover, air pollution, and several other surface characteristics (Zha, 2012; Weng, 2004). Spaceborne thermal remote sensing techniques have been developed and successfully applied to map UHI in various urban areas (Kato, 2006; Streutker, 2003; Tran, 2006; Voogt and Oke, 2003). Thermal remote sensing data can be used to study the difference between midnight and noon temperature measurements of Las Vegas.

The measured radiance in the thermal infrared spectrum can be converted to a surface temperature using Planck's Law at each cell of the captured image. Surface temperature maps will need to be compared with other UHI factors such as percent impervious surface area, vegetation coverage, and sampled air temperatures to generate a reliable UHI model of the area. High resolution images can provide continuous data over a surface, but the images can only be captured at discrete times because the remote sensing device does not typically remain stationary over the Earth's surface. One of the main difficulties with using remote sensing equipment is that the device can only detect upward radiance from visible surfaces. Only two dimensional surfaces can be rendered and objects such as clouds can block radiance from the surface causing inaccurate data recordings.

Remotely sensed images used in this analysis were provided by the Landsat program. The Landsat program is a corroborative effort between the U.S. Geological Survey (USGS) and the National Aeronautics and Space Administration (NASA) to gather satellite remote sensed spectral images of the Earth's surface. The first of seven satellites was launched July 23, 1972. Landsat satellites 1 through 3 captured images with two different devices: The Return Beam Vidicon (RBV) camera system and the Multispectral Scanner (MSS). The satellite relayed the captured data through seven channels called bands. The first three bands were designated to each of the three RBV television cameras that capture panchromatic images within the 0.5 to 0.75 μm spectral range. The latter four bands are for the MSS which has moving parts that scans strips of the Earth. Each of the bands is able to detect a portion of the visible and infrared spectrums. Band 4 imaged green radiance (0.5 to 0.6 μm), band 5 imaged red radiance (0.6 to 0.7 μm), and bands 6 and 7 detected infrared (0.7 to 0.8 μm and 0.8 to 1.1 μm , respectively). Each band RBV was intended to be primary imaging device with MSS being an experimental capturing method. The moving parts of the MSS were considered to be a liability, but apparent superiority of the MSS data from the first captured images and the failure of the RBV shortly after Landsat 1 launch made MSS the more preferable imaging method. Thermal infrared (TIR) imaging was included with the MSS for the Landsat 3 and with Thematic Mapper (TM) for the Landsat 5 (Chander et al., 2009).

2.5 Las Vegas Valley

Urban influence on temperatures is dependent on climate characteristics of the region (Taha, 1997). This means temperature change over a city area differs between

climate locations. Few studies have been performed in determining the effect of UHI in Las Vegas.

Las Vegas Metropolitan region is defined by the BLM disposal boundary indicating land available for sale and development to the public. The disposal boundary consists of City of Las Vegas, City of North Las Vegas, Henderson, and Nellis Air Force Base (See Figure 2). The remaining land within the disposal boundary is unclaimed by any local municipalities and is referred to as unincorporated Clark County. The study area analyzed in this thesis is a rectangular boundary that includes the BLM disposal boundary.

Las Vegas means “the meadows” or “fertile lowlands” in Spanish. This name refers to the natural springs charged by an expansive aquifer that covers a majority of the valley. This reliable water source became a popular stopping point for travelers heading towards Los Angeles or for settlers seeking to farm or mine the land between 1850 and 1900.

On May 15, 1905, 110 acres was auctioned off establishing Las Vegas city area. A city government was established by 1911 with a city population just over 800 people. Las Vegas steadily grows to 5,165 residents by 1930. The completion of Boulder Dam in 1935, establishment of industrial and military complexes during WWII in the 1940’s, and Las Vegas’ notoriety as an entertainment capitol encouraged an accelerated population growth rate between 1945 and 2010.

The population of the Las Vegas between 1990 and 2011 is graphed in Figure 3 (Comprehensive planning demographics). The metropolis averaged a 5.6% population

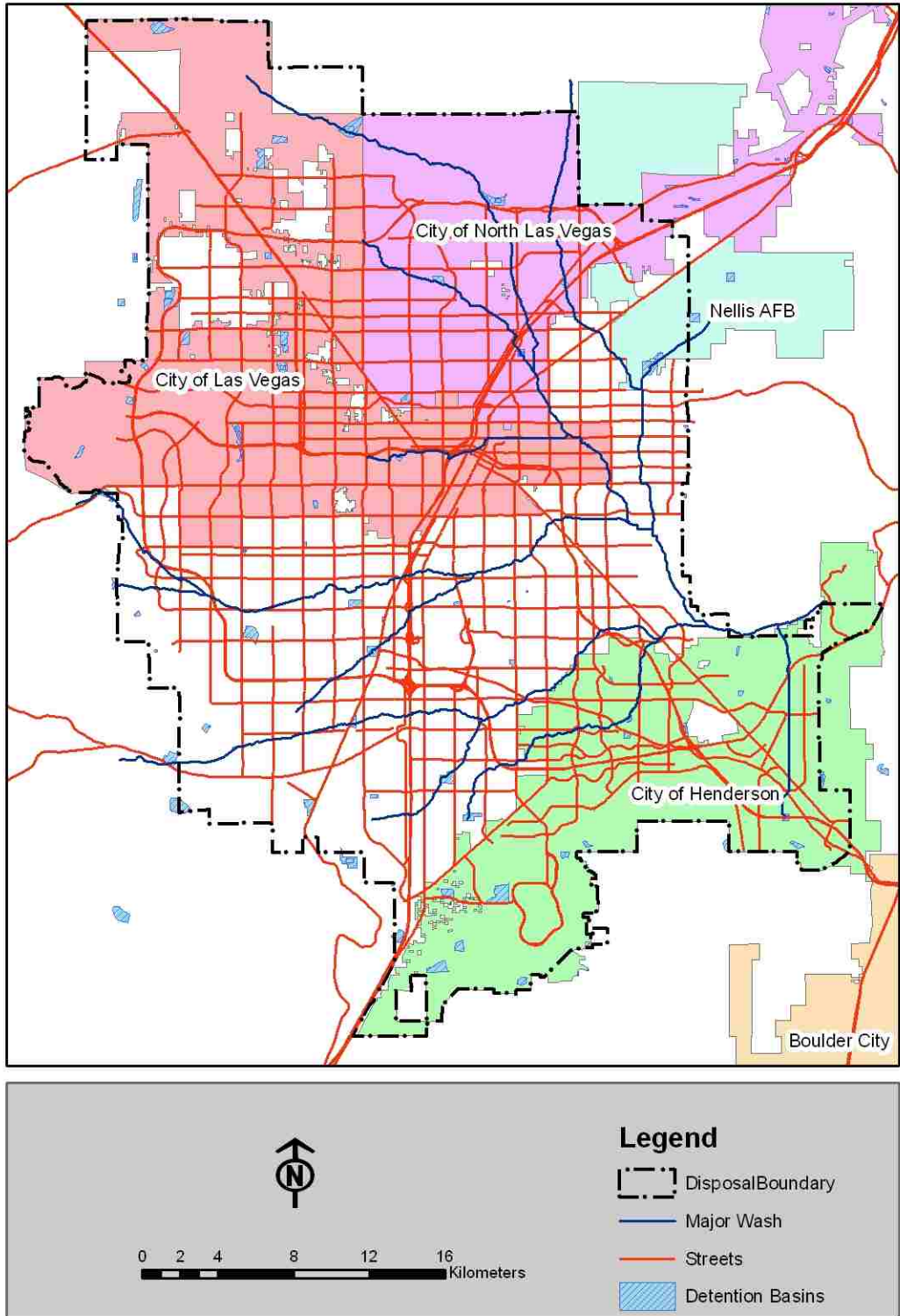


Figure 2: Las Vegas disposal boundary and city locations.

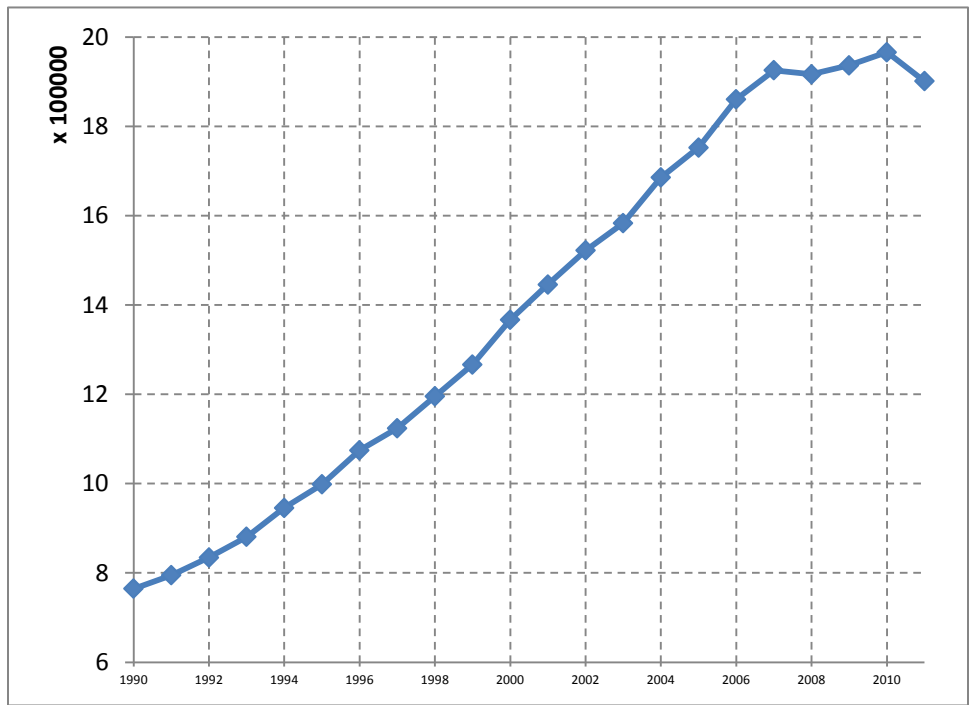


Figure 3: Las Vegas population growth between 1990-2011.

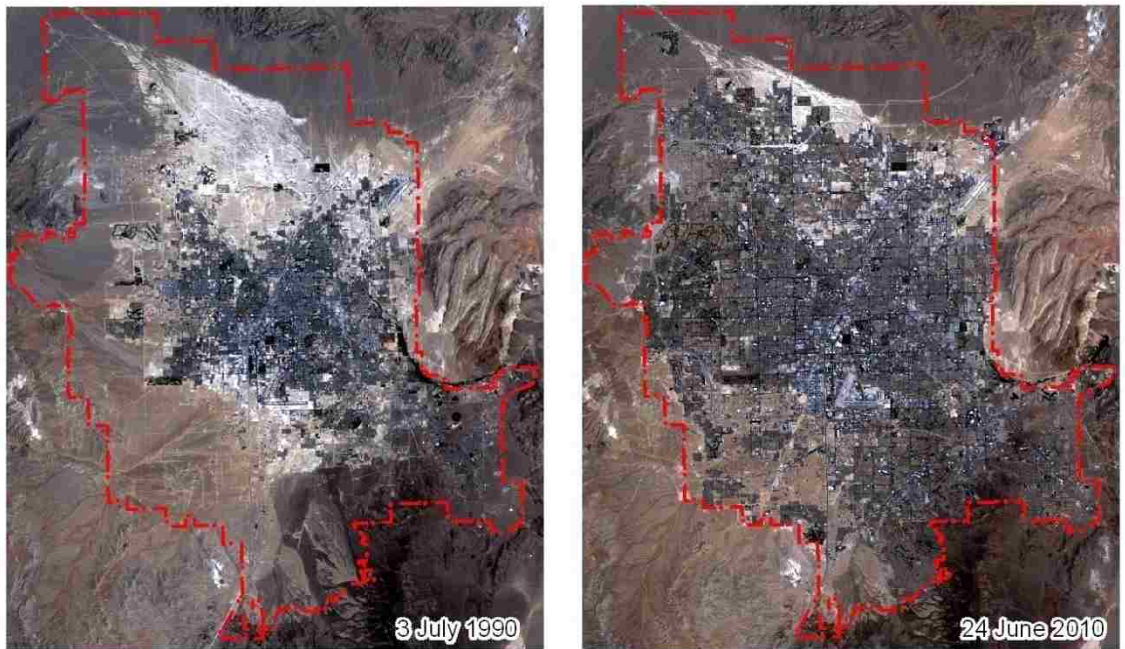


Figure 4: Comparison of 1990 vs. 2010 aerial view of Las Vegas.

growth per year between 1990 and 2007 reaching a peak population near 2 million people by 2010. Figure 4 gives a birds-eye perspective of the Las Vegas area during the summers of 1990 and 2010. The images depict urban land coverage expansion to the north, west, and south during the 20 year period that increases the metropolis area by approximately 90%. This consistent expansion of urban area in Las Vegas over a short period of time provides an opportunity to detect gradual temperature changes influenced by an increasing presence of urban materials.

A student paper from California Polytechnic State University has presented the signs of UHI development in Las Vegas by comparing temperatures of two weather stations located in an urban and rural setting (Remar, 2010). Remar chose an urban weather station near central Las Vegas maintained by McCarran Airport and a rural station monitoring temperatures in the Valley of Fire state park northeast of Las Vegas. Both stations have been recording temperature data before 1970 to the present. Comparison of temperature time series at these two locations has suggested two climate behaviors for the area. Remar first noted that rural temperatures at the Valley of Fire weather station are consistently higher than the temperatures at central Las Vegas. Secondly, time series plots of the average maximum and minimum temperature of a given month over the last 40 years shows differing trends between the two regions. Both the maximum and minimum temperatures in the rural region appear to exhibit relatively consistent behavior. For the urban weather station, the maximum temperatures also showed little variation in behavior over time, but the plotted average minimum temperature for a month displayed a noticeable increasing trend. These results suggest

that nighttime temperatures in Las Vegas are rising as the city expands, although there is no indication from the analysis of the location, size, or intensity of the heat islands.

Mapping UHI development in Las Vegas directly from weather station temperature data is a difficult task because of the available number of near surface temperature data during this time period of urban growth. Few weather stations consistently recorded air temperatures for public use between 1990 and 2010 in Las Vegas. The scarcity of long term stations and station locations reduces the reliability and accuracy of any interpolated UHI map from temperature data of the area. The best obtainable results that can be obtained are an approximation of overall temperature trend changes caused by urban modifications (Oke, 1978).

Researchers are starting to include remotely sensed surface temperature data in their analyses of geographical development of heat island in urban regions. Remote sensing images are rich with continuous geographical data and satellite programs have been collecting images periodically for more than 30 years for the entire Las Vegas region. Even though satellites average about two images per month of an area and are very sensitive to weather conditions, remote sensed images are very useful for geographical analysis of UHI.

George Xian and Mike Crane analyzed surface thermal characteristics in Tampa Bay, Florida and Las Vegas, Nevada using remote sensed images from USGS Landsat program (Xian et al., 2006). Their research compared changes in surface temperature and vegetation density for varying ranges of percent impervious surface area between two Landsat images captured 1995 and 2002 for Tampa Bay, and 1984 and 2002 for Las

Vegas. The conclusions of the paper evaluate the effects of land use and land cover on urban climates. Xian and Crane's results showed that Tampa Bay and Las Vegas have differing surface temperature trends as impervious surface area increases. Tampa Bay surface temperatures increased between 1995 and 2002 while Las Vegas surface layer experienced a slight cooling trend in built-up areas between 1984 and 2002. Although, the temperature difference in Las Vegas is greater for areas with minimal impervious surfaces.

Comparison of impervious surface area with NDVI data indicate that changes in surface temperature in both cities corresponded to the inverse change of vegetation cover. The Tampa Bay environment naturally consists of dense foliage that maintains cool surface temperatures. Urbanization of Tampa Bay replaces natural rural surfaces with impervious materials that are more likely to attain higher temperatures. Las Vegas rural surfaces are composed of sparse shrubs and desert soils with characteristics similar to concrete. NDVI analysis of Las Vegas indicates that urban build-up activity increases the presence of green surface area wherever impervious surfaces are not present.

Xian (2008) has shown that Las Vegas area showed a slight decline in surface temperature as impervious area transitions from low to medium urban density. This surface temperature trend reverses direction and begins to increase at a significant rate when impervious area becomes greater than 50 percent. This suggests that high impervious surface area counteracts the cooling effect of vegetation by reducing the available area for green surfaces. Xian's previous work (Xian et al., 2006) also shows that the cooling effect between 1984 and 2002 in Las Vegas is reduced as the impervious surface area increases.

Xian et al. concluded that surface temperature is mildly influenced by the land coverage of impervious and green surface composition of an area. The use of remote sensed images in UHI analysis of the surface layer was able to quantify temperature changes and the area of influence based on ground characteristics. It is noted that these studies are unable to connect surface temperatures with nighttime air temperature trends. Especially since satellite images are captured during daytime hours and can only provide information about the surface layer.

Urban materials and surfaces may be cooler than native desert soils in the daytime, but developed land may still have negative effects on Las Vegas' evening air temperatures (Arnfield, 2003). Continued research should examine ways to correlate station data with remote images to study stronger relationships between surface characteristics and air temperature trends for a geographical area.

This review of literature shows that urban heat island effect is a serious problem in cities. As Las Vegas has grown, several parts of the city are experiencing fluctuations in temperature trends that need to be studied and understood. Few studies have addressed the temperature trends in Las Vegas. Las Vegas, being in an arid region with limited water resources, faces challenges of balancing urban forestry with water consumption. This thesis presents a study of temperature trends in Las Vegas to understand the temperature response to urban development.

This thesis contributes to the existing knowledge of urban temperature trends in the following ways. Temperature trends in Las Vegas are linked to urban expansion by modeling temperature data from 14 weather stations and several remote sensing images

over a 10 year time period. Relationships were developed for surface and air temperatures at 30 weather station locations using the station's temperature data and remote sensing images. A new measure of urban heat island intensity is devised that is based on the surface and air temperature relationship.

CHAPTER 3: Data and Methods

This chapter outlines the steps used to analyze UHI formation in Las Vegas and describes the methods used to perform time series and data correlation analyses. The described methods are categorized into three sections. The first section provides temporal temperature modeling methods to evaluate temperature trends in the Las Vegas area. The next section describes the correlation process to associate land surface temperature with air temperature observations. The relationship is used to create images that are used to convert temperatures at the surface layer into approximate canopy layer temperatures at noon and midnight for the day the image was captured. The converted images are compared to determine areas where UHI are most likely to form. The final section applies methods to identify land use and land cover from raster images and other third party files. Results will be used to correlate surface material cover of an area with UHI size and strength.

3.1 Research Approach

In this research, ground measurements of air temperature and remote sensing measurements of lands surface temperature were used to analyze the spatio-temporal thermal behavior of Las Vegas urban area. Ground based temperature measurements are used to perform trend analysis of temperature time series. Statistical relationships are developed between air temperature and land surface temperature that are used to estimate the midnight and noon temperature from the remotely sensed temperature data. Since urban heat islands have high nighttime temperature, we define urban heat island intensity (UHII) as the difference between the midnight and noon temperature. Spatial estimates of

UHII are mapped and used to identify the urban heat islands. Landuse and tree canopy maps of Las Vegas are used for comparison in this analysis. Comparison of surface radiance at different wavelengths can reveal high resolution surface characteristics over a region.

Landcover maps, urban/suburban boundaries, urban zoning data, remote sensing data, and meteorological data are used to identify the urban heat islands in Las Vegas Valley. The overarching goal of the project is to facilitate identification of potential areas for planting trees in the valley to reduce in the heat island effect. As mentioned earlier, UHII is measured as the difference of midnight and noon temperature. This is based on the observation that the urban heat islands that retain heat during the night do not cool down sufficiently and thus have high nighttime temperatures. Since midnight and noon temperature data of the whole valley is not available, it is estimated by developing regression relations between ground measurements and remote sensing thermal images. The research approach used in this thesis is shown as a flow chart in Figure 5.

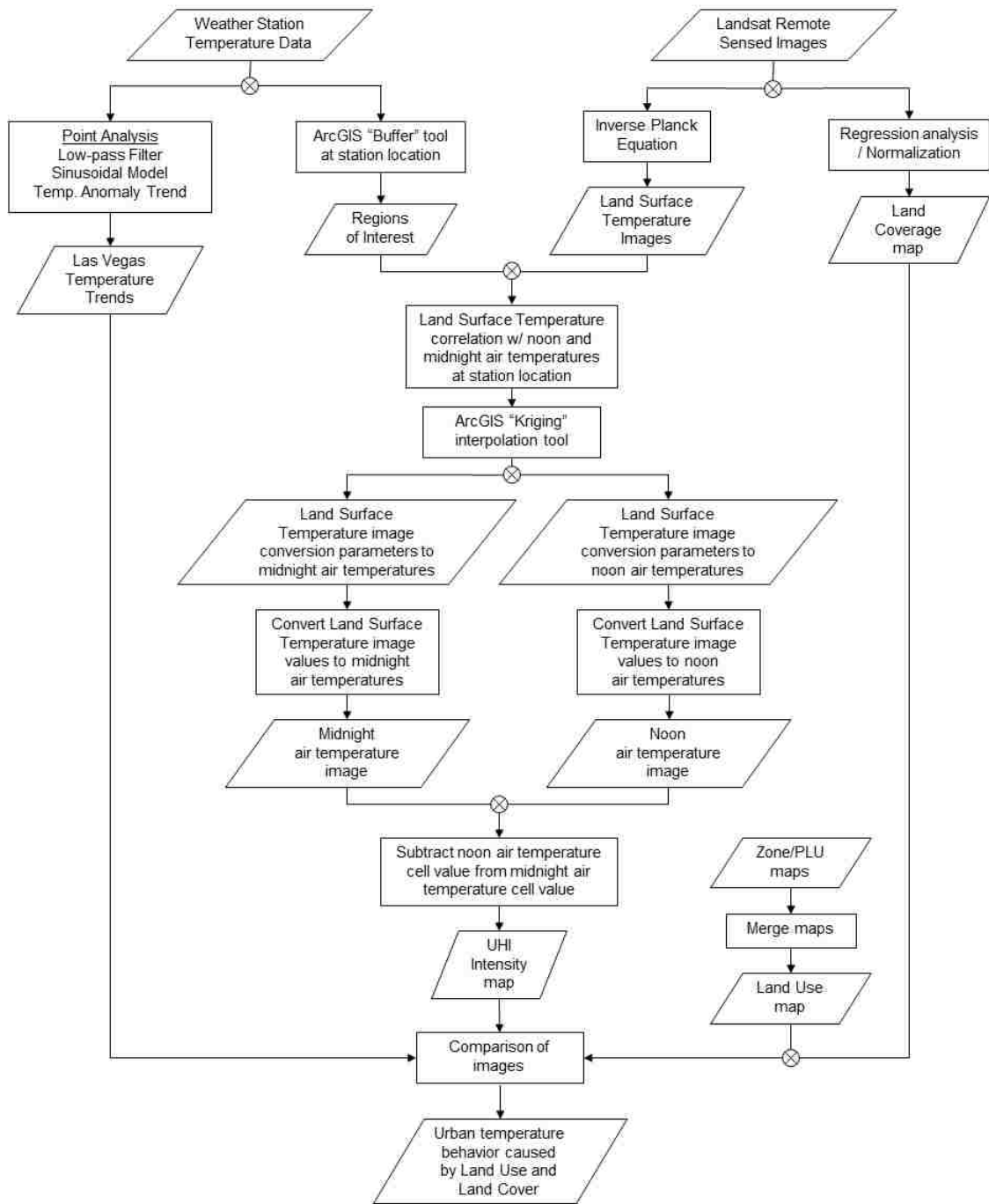


Figure 5: Research method flowchart.

3.2 Data

This research is performed using near surface air temperatures observed at several points in the Las Vegas valley and land surface temperatures from remotely sensed thermal infrared images.

3.2.1 Meteorological Temperature Measurements

Near surface air temperatures are provided by a commercial weather service website called the Weather Underground at <http://www.wunderground.com/wundermap/>. This analysis referenced temperature records of 32 Weather Underground PWS, 3 airport monitored weather stations, and 1 military air force base weather station in the Las Vegas area from the Weather Underground webpage. Java script programs were used to download near surface temperature observations for all Weather Underground meteorological station. Time stamps recorded in Pacific Standard Time (PST) were converted to Coordinated Universal Time (UTC) with consideration of Pacific daylight savings time (PDT). Weather underground also provides station latitude/longitude locations in degrees, minute, and seconds with elevation in feet. Station name, ID, location, and elevation were recorded in an Excel spreadsheet and saved as a CSV file.

Table 1 lists weather station designations, time period of the collected temperature data, and current land use based on visual inspection of the area. Previous studies have shown a strong correlation of UHI and LST with LULC (Chen, 2006; Lo, 1997; Stone 2006; Yuan, 2006). Stewart and Oke have suggested Local Climate Zone (LCZ) definitions based on urban surface geometry and composition (Stewart and Oke, 2012).

Table 1: Weather Underground Station List

No.	Name	Date Period	LCZ
1	Henderson Executive Airport	2002 - 2012	9F
2	McCarren Airport, Las Vegas	1948 - 2012	8E
3	Nellis AFB	1942 - 2012	8E
4	Seven Hills	2006 - 2011	9F
5	MacDonald Ranch	2006 - 2011	9F
6	Bailes Home Weather	2009 - 2011	9F
7	Sun City Anthem	2006 - 2011	6F
8	Whitney Ranch-Residential	2009 - 2011	6E
9	Legacy Golf Course Area	2004 - 2011	6E
10	Rhodes Ranch	2002 - 2011	9C
11	Photo Patterns, East	2004 - 2011	8E
12	Neon Desert Weather, East Las Vegas	2004 - 2011	6E
13	NW Spring Valley	2005 - 2011	6C
14	Photo Patterns, West	2005 - 2011	3F
15	Centennial Hills	2008 - 2011	6E
16	Southern Highlands	2010 - 2011	9C
17	Elkhorn Springs	2009 - 2011	3E
18	Palomino Estates	2001 - 2011	3C
19	Weather Dog House	2009 - 2011	3E
20	Aliante	2009 - 2011	6F
21	North Las Vegas Airport	1997 - 2012	8E
22	Angel Park NV US Las Vegas	2007 - 2011	9C
23	Henderson NV US	2007 - 2011	6F
24	Henderson NV US CEMP	2007 - 2011	6F
25	Las Vegas NV US CEMP, North	2007 - 2011	5E
26	Las Vegas NV US CEMP, South	2010 - 2011	9F
27	Las Vegas NV US	2010 - 2011	9F
28	Summerlin West NV US Las Vegas	2010 - 2011	F
29	Apex NV US UPR	2009 - 2011	9F
30	Arden NV US UPR	2007 - 2011	9F

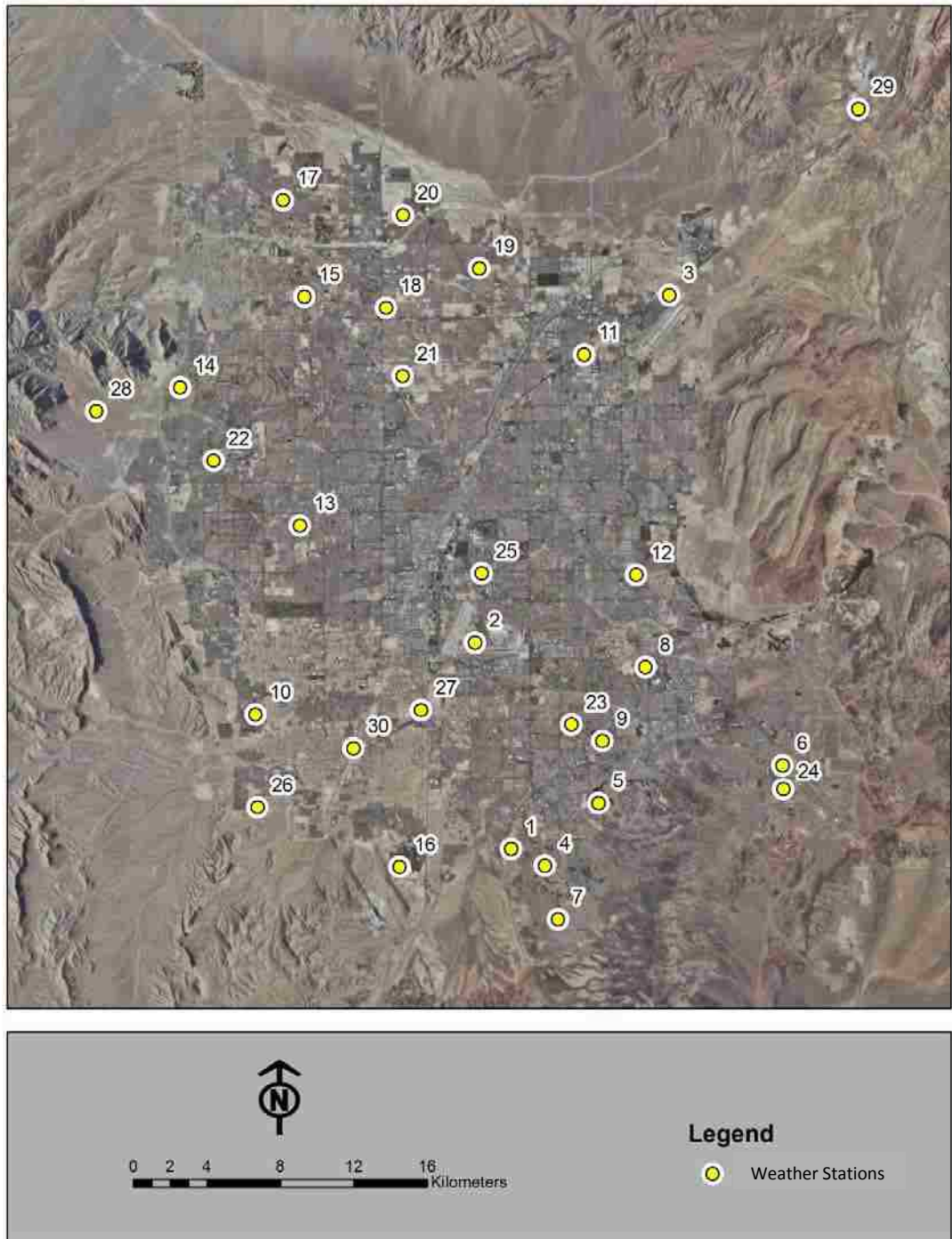


Figure 6: Weather station locations in Las Vegas valley.

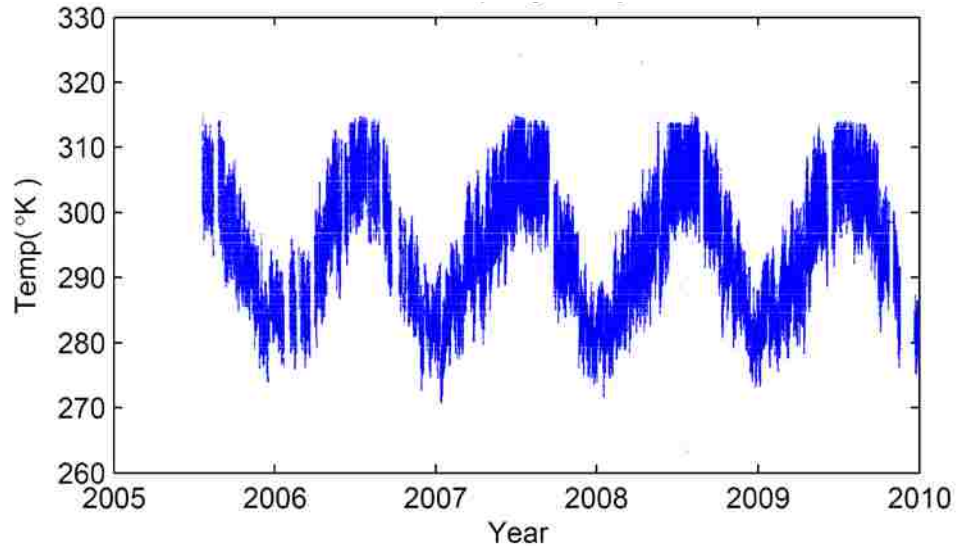


Figure 7: Sample plot of temperature data vs. time for weather station 13.

LCZ classifications with description are listed in Appendix B. Figure 6 shows the map of station locations in the Las Vegas valley.

Long term temperature variations follow a sinusoidal pattern mainly influenced by the direction of tilt of the planet with respects to the sun. Sample raw data from a weather station located in the northwest Spring Valley area is presented in Figure 7 to show typical temperature variations in the region. Las Vegas area experiences cooler temperatures that range from 275 K and 295 K between the winter months of December and March when the hemisphere is tilted away from the sun. The temperatures transition to a warmer range between 295 K and 315 K during the summer months between June and August when the Earth is tilted towards the sun.

The hemisphere tilted away from the sun experiences shorter days which reduces the total solar energy that enters the canopy layer . The sunlight also travels through a thicker layer of the atmosphere due to the sun follwing a non-perpendicular path with reference to the region surface. The majority of the heat energy is diffused into the upper

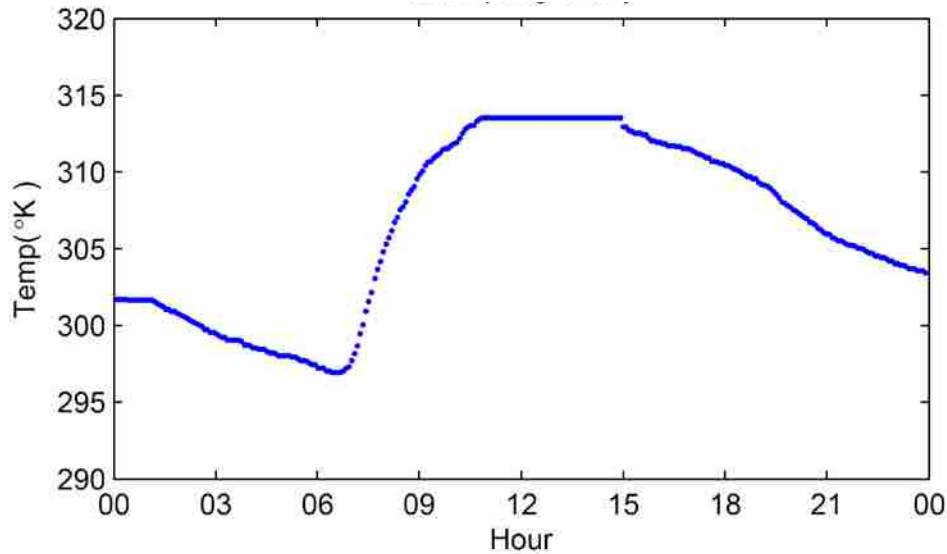


Figure 8: Diurnal temperature variation for station 13 on Aug. 27, 2010.

atmosphere before reaching the surface. Also, the remaining heat energy will reach the surface at an oblique angle which increases the energy reflected back to the atmosphere during the day and reduces the energy absorbed by the surface.

Diurnal temperature variation is due to the rising and setting of the sun. A single day of temperature observations from the northwest Spring Valley meteorological station is shown in Figure 8 to depict typical diurnal temperature behavior. When the sun rises, morning temperature quickly increase between 6am and 12pm to peak around 2pm. During sunset and the evening hours, the air gradually cools until sunrise. The increase in temperature is a direct result of the sun supplying heat energy to the canopy layer. The cooling rate of canopy layer temperatures in the evening is a combination of the cooler upper atmosphere replacing the warmer lower atmosphere and the flow of heat energy from the surfaces to the canopy layer.

3.2.2 Remote Sensed Images

Remote sensed raster images were downloaded from the US Geological Survey (USGS) website at <http://glovis.usgs.gov/> available in GeoTIFF format. The raster images used in this research are a product from the Landsat program between 1984 and 2011 from the fifth generation satellite which comprises of approximately 360 images. Each image data package contains 7 GeoTIFF images corresponding to 7 bandwidths. Each bandwidth detects radiance within a unique portion of the light spectrum. The data package also contains a metadata text file containing conversion factors to convert raster cell digital values between 1 and 255 to radiance (watts/[m²·ster·µm]). Raster pixel resolution is 30 meters except for raster images from band 6 (thermal infrared) which have a pixel resolution of 120 meters. Raster values of each image are converted using the following equation.

$$CV = \frac{LMAX-LMIN}{QCALMAX-QCALMIN} \cdot (DN - QCALMIN) + LMIN \quad (2)$$

LMIN and LMAX are the radiance range for the corresponding band that can be referenced from the metadata text file included in the download package. QCALMIN and QCALMAX are 1 and 255 respectively which represents the digital number range to maximize cell value storage of one byte per cell. DN is the input digital number and CV is the output cell value in radiance.

Land Surface Temperature

Several of the methods described in this chapter analyze land surface temperature raster images calculated from the thermal infrared band. Thermal infrared images

indicate the spectral radiance emitted from a surface that occur between the wave lengths 10.4 μm and 12.5 μm . Thermal spectral radiance emitted from a surface within this spectral range can be converted into radiation temperatures by using an equation based on the inverse of Planck's equation:

$$T = \frac{K_2}{\ln\left(K_1 \cdot \frac{\varepsilon}{CV_{TIR}} + 1\right)} \quad (3)$$

Where T is the temperature in Kelvin, ε is the emissivity (typically 0.95), and CV is the cell value of the thermal infrared image. K1 and K2 are calculated constants unique to the device used. Provided K values for K1 and K2 are 607.76 and 1260.56, respectively, for the Thematic Mapper data used in this research.

Normalized Difference Vegetation Index

Dense vegetation cools the surface and air temperatures of the immediate surroundings with evapotranspiration and supplying shade (Weng, 2004). Percent area of vegetation cover is one of the main factors of UHI development and can be determined with the NDVI. NDVI is based on the principle that vegetation absorbs solar radiation within the visible spectrum, but scatters and reflects energy within the infrared region. Because of this, plants appear 'dark' in the red spectrum and are 'bright' in the infrared spectrum. The NDVI image is constructed by finding the normalized difference between these two spectral regions.

$$NDVI = \frac{(CV_{NIR} - CV_{RED})}{(CV_{NIR} + CV_{RED})} \quad (4)$$

The greater the NDVI value of the cell, the higher the density of vegetation in that area. Cell values between 0.3 and 1 are considered to be covered in significant amounts of vegetation.

3.2.3 Zoning and Planned Land Use Boundaries

Las Vegas valley zoning map of the planned landuse is prepared by merging the land use boundaries and government zones across all the cities. Each city has developed a zoning map with custom building codes of landuse characteristics. These maps were merged to create a unified landuse map of Las Vegas. GIS layers of the zoning maps were accessible at the Clark County GIS Management Office (GISMO) website (GISMO, 2013). The data used for preparing the zoning map is listed below.

In order to understand how the UHII is related to various zones of Las Vegas, and integrated landuse map was created by combing the planed landuse maps of all areas acquired from GISMO. The Las Vegas zoning map was prepared by merging the landuse maps of the individual cities. In the merging process, careful attention was given to the merging of the different classification schemes used by the cities.

The zoning definitions contained in the building codes are grouped into residential, commercial, industrial, public facilities, open lands, and right of way categories. Any map types not designated within the building codes are classified based on best judgment. A combined table was created as shown in the appendix A.

Shapefiles downloaded from GISMO were opened in ArcMap map document. The attribute tables were then compared to zone map PDF's for accuracy. Shapefiles that matched the PDF's the best were selected to build the valley wide planned land use

Table 2: Referenced Figures and Shapefiles Used to Create a Unified Land Use Map of Las Vegas

<p><u>City of Henderson</u> Existing Zoning map by Geographic Information Services created Sept. 2011. HDZoning shapefile by Community Development GIS adopted July 20, 2010.</p>
<p><u>City of Las Vegas</u> City of Las Vegas Zoning map by Planning & Development Dept. created July 11, 2011. CLV_Zoning shapefile – File description does not include publisher and date within metadata information.</p>
<p><u>City of North Las Vegas</u> Zoning map by Community Development Dept. Planning and Zoning Division GIS Services created March 31, 2011 NLVZONE_P shapefile – File description does not include publisher and date within metadata information.</p>
<p><u>Clark County (Material created by Comprehensive Planning Dept.)</u> Enterprise Planning Area map created Nov. 4, 2009 CC_ENTPLU_p shapefile created Sept. 2, 2009 Lone Mountain Planned Land Use map created Oct. 14, 2008 CC_LMPLU_p shapefile created Sept. 17, 2008 Northeast County Planned Land Use map created Oct. 4 2006 CC_NEPLU_p shapefile created Sept. 6, 2006 Northwest County Planned Land Use map created April 10, 2008 CC_NWPLU_p shapefile created Nov. 7, 2007 South County Planned Land Use map created Feb. 8, 2007 CC_SCPLU_p shapefile created Dec. 6, 1994 Spring Valley Planning Area map created Nov 4, 2009 CC_SPVPLU_p shapefile created Dec. 10 2004 Sunrise Manor Planning Area map created Oct. 11 2010 CC_SRMPLU_p shapefile created Jan. 18, 2006 Summerlin South Planned Land Use map created April 18, 2007 CC_SUMPLU_p shapefile created May 28, 2003 Whitney Planned Land Use map created May 15, 2007 CC_WHPLU_p shapefile March 21, 2007 Winchester and Paradise Planned Land Use map created Sept. 8, 2010 CC_WPPLU_p shapefile created Aug. 3, 2005</p>

shapefile. The polygons in each shapefile were exported into separate files based on their zone classification. A column labeled 'ZONE_CODE' was added to each attribute table of the exported shapefiles and populated depending on the shapefile zone classification. There were no agricultural (B6) areas identified in the Las Vegas valley study area. Below is the list of zones in the combined landuse map.

AFB – Nellis Air Force Base

B1 – Residential

B2 – Commercial

B3 – Industrial

B4 – Public Use / Facilities

B5 – Open Land

B6 – Agricultural

B7 – Right of Way (ROW)

UZ – Unclassified Zone or ROW

All exported files are then combined (merged) into a single file and then clipped to the masking boundary. In the final step, union of zoning shapefile and masking boundary was performed to fill in the unclassified areas. Data was cleaned up by removing the extra columns from the shapefile. The final map is shown in Figure 9.

3.2.4 Southern Nevada Water Authority 2006 Canopy Data

Southern Nevada Water Authority (SNWA) (Brandt, 2008) used remote sensing data and GIS techniques to develop a vegetation canopy cover map of Las Vegas. Moderate resolution Landsat and high resolution color infrared (CIR) imagery were used to classify trees, turf, and shadows. A final canopy dataset was prepared with an overall accuracy of 92%. In this research, we relate this data to the spatial behavior of urban heat island intensity.

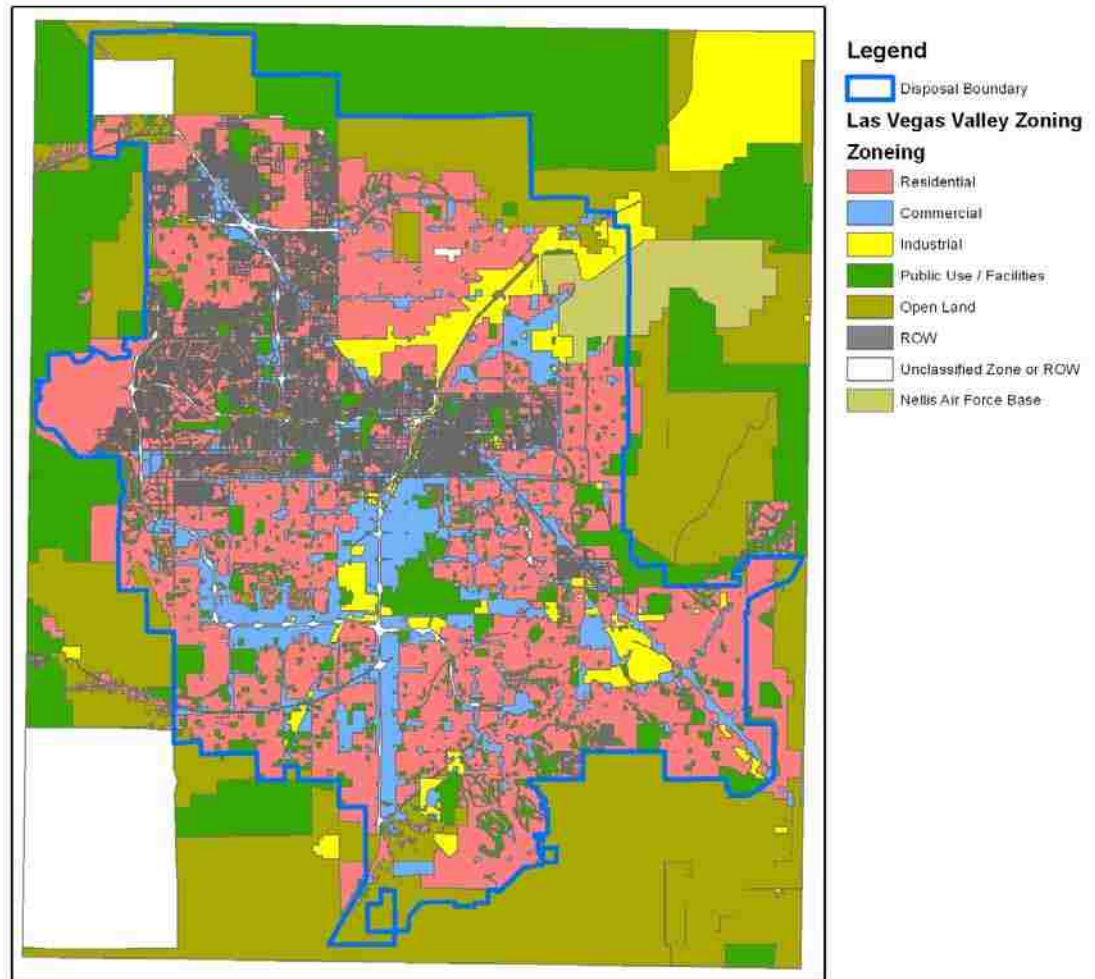


Figure 9: Unified landuse map of Las Vegas.

3.3 Temperature Trend Analysis at Weather Station Locations

This section describes the methods applied to temperature time series to obtain long term temperature trends at selected points in the Las Vegas area. Three methods were selected and applied to model the temperature data trends. These methods are a low-pass filter, sinusoidal model, and temperature anomaly trend. These analysis methods were selected based on their ability to handle the periodic temperature behavior to obtain a long term temperature change. The results are used to approximate the temperature

change rate at each weather station. Root mean square error was calculated for each method to assess the accuracy of the output. Data criteria were applied to station observations to control result quality.

Short term trend analysis was performed with temperature data that falls between 2006 and 2011. Long term temperature analysis performed at stations having data sets of 10 years or greater. The point based temperature trend obtained is interpolated to obtain trend surfaces for the study area. The inverse distance weighted (IDW) interpolation technique is used to create these trend surface maps.

The interpolated temperature trend maps were associated with ground cover characteristics to identify any surface properties that influence local long term temperature trends. Data sets used to approximate surface properties are planned land use maps from local government entities and satellite remote sensed images obtained from the Landsat program. Some treatment of the original data was required to create surface property images for comparison to the long term temperature trend surfaces. The procedures to process the images are given at the end of this section.

3.3.1 Low-pass Filter Approach

A low-pass filter removes high frequency data noise to reveal underlying low frequency trends of data sets. This method has several real world applications including smoothing images and cleaning audio or electrical signals. Removing the high frequency from a data set is accomplished by applying

$$\bar{T}_k = \frac{1}{n} \cdot \sum_{i=-n/2}^{n/2} T_{k+i} \quad (5)$$

where n is the window size and k is the index at which the average is computed. \bar{T}_k is the average temperature computed from index values $k - n/2$ to $k + n/2$. This low-pass filter method is called a moving average low-pass filter. Moving average low-pass filter has been used frequently in research to reduce data noise to improve data analysis (Ahani, 2012; Laory, 2011).

The main parameter selection of this method is deciding an appropriate window size. The larger the window size the smoother the data becomes. Application of trial and error and rounding results to a common time period has shown that a window size that covers 31 days, or one month, adequately removes the diurnal cycles while leaving sufficient detail to analyze the annual temperature behavior. This allows for trend analysis of the annual behavior while minimizing influences from diurnal trends. The moving average method is an effective way of removing short term trends for long term analysis, but there is no quantifiable parameter output that can be used to base research conclusions.

There are other methods that are able to separate long term temperature behavior from a data set and express the results in numeric form. Sinusoidal modeling is one such method since annual temperature behavior typically follows a pattern similar to a sine wave.

3.3.2 Sinusoidal Model Approach

Sinusoidal modeling evaluates the parameters for a sine wave function that will be a best match of the data set behavior. Sinusoidal modeling has been used to analyze sound wave, biomedical signals, environment behavior, and several other research areas (Yang, 2009; Sherman, 2004; Laas 2012). The annual variation of the temperature data has an annual periodical pattern resembling a sine wave. The sinusoidal model method is used to estimate long term temperature behavior at a weather station.

Temperature annual variation is modeled as

$$T(t) = b + m \cdot t + A \cdot \sin(\omega \cdot t + \phi) + e \quad (6)$$

where t is the time expressed in days, T is the air temperature at time t , and e is the error of the observed temperature from the modeled sine curve. The other parameters indicate the modeled sine function characteristics and linear trend. The main parameters of importance are m for the temperature rate of change, A representing the temperature amplitude, and ω as the angular frequency of the sine wave. The annual temperature pattern repeats once every year. Therefore, the angular frequency is approximately equal to $2 \cdot \pi/366$ radians per day or about 0.017 rad/day. The temperature rate of change and amplitude are unknown and are estimated by this method.

The parameters b and ϕ are the y-intercept and the phase shift, respectively. The y-intercept indicates where an imaginary line drawn laterally through the center of the sine wave function will intersect the y-axis. The phase shift signifies the function offset from the standard sine function. Both parameter values are related to the sine wave position with the y-axis and have no significant relation with long term temperature

trends. Also, the y-intercept and phase shift values will not be consistent between serial date numbering procedures while the amplitude and slope results will essentially remain unchanged. The y-intercept and phase shift results will not be reported for these two reasons.

The model fitting process chosen for this method involves solving a linear system of equations to find the unknown coefficients using a least squares error method. This is an accepted research approach to find the best fit coefficients of a linear system used by most statistical analyses (Keller-McNulty 1987).

The first part of the modeling process is to create a linear equation from the sinusoidal model function. This requires the expansion of the trigonometric portion of the Equation 7 to bring the unknown ϕ into the term coefficient. Equation 8 demonstrates the expansion process that brings the phase portion outside of the sine operation in Equation 8.

$$A \cdot \sin(\omega \cdot t + \phi) =$$

$$A \cdot \cos(\phi) \cdot \sin(\omega \cdot t) + A \cdot \sin(\phi) \cdot \cos(\omega \cdot t) \quad (7)$$

The unknown portions of each term in Equation 8 are combined into two simplified coefficient. The simplified equation and coefficient definitions are given as

$$A \cdot \sin(\omega \cdot t + \phi) = C_1 \cdot \sin(\omega \cdot t) + C_2 \cdot \cos(\omega \cdot t) \quad (8)$$

where,

$$C_1 = A \cdot \cos(\phi) \text{ and } C_2 = A \cdot \sin(\phi)$$

Applying the expansion process to Equation 7 produces the following modified sinusoidal model function. This function is the form used in the fitting process.

$$T(t) = b + m \cdot t + C_1 \cdot \sin(\omega \cdot t) + C_2 \cdot \cos(\omega \cdot t) + e \quad (9)$$

For a temperature data set, Equation 10 is applied to each temperature measurement $T_i(t_i)$ made at time t_i to construct a linear system shown in the following equation.

$$\mathbf{X} \cdot \mathbf{C} = \mathbf{T} \quad (10)$$

where,

\mathbf{T} is a $n \times 1$ matrix of temperature observations, $[T_1 \ T_2 \ \dots \ T_n]^T$.

\mathbf{X} is a $n \times 4$ matrix of values calculated from Eq. 10 terms such that

$$\mathbf{X} = \begin{bmatrix} 1 & t_1 & \sin(\omega \cdot t_1) & \cos(\omega \cdot t_1) \\ 1 & t_2 & \sin(\omega \cdot t_2) & \cos(\omega \cdot t_2) \\ \vdots & \vdots & \vdots & \vdots \\ 1 & t_n & \sin(\omega \cdot t_n) & \cos(\omega \cdot t_n) \end{bmatrix}$$

\mathbf{C} is a 4×1 matrix of the model parameters, $[b \ m \ C_1 \ C_2]^T$.

The coefficients are found by solving the linear system for matrix \mathbf{C} by finding the inverse of matrix \mathbf{X} , depicted as \mathbf{X}^\dagger in Equation 12, and multiplying it by matrix \mathbf{T} .

$$\mathbf{C} = \mathbf{X}^\dagger \cdot \mathbf{T} \quad (11)$$

An inversion of a matrix can only truly be performed on a square nonsingular matrix. A generalized inverse of matrix \mathbf{X} can be evaluated by finding what is called the pseudo-

inverse which results in an inverse that will provide a linear least square solution to Equation 11 (Keller-McNulty 1987). The pseudo-inverse is given by

$$\mathbf{X}^\dagger = (\mathbf{X}^T \cdot \mathbf{X})^{-1} \cdot \mathbf{X}^T \quad (12)$$

Applying the pseudo-inverse to the Equation 11 creates Equation 14 which will find the coefficients of the sinusoidal model.

$$\mathbf{C} = ((\mathbf{X}^T \cdot \mathbf{X})^{-1} \cdot \mathbf{X}^T) \cdot \mathbf{T} \quad (13)$$

The amplitude and phase shift can be derived from C_1 and C_2 coefficients. These model parameters can be obtained with equations 15 and 16.

$$A = \sqrt{C_1^2 + C_2^2} \quad (14)$$

$$\phi = \tan^{-1}\left(\frac{C_2}{C_1}\right) \quad (15)$$

Using the coefficient obtained from the least squares error method will approximate the sinusoidal model of the temperature data set. The annual periodic variation is removed from the model to obtain long term trend, m , from the remaining residual temperature.

3.3.3 Temperature Anomaly Trend Approach

In this method, the annual cycle of temperature is removed through a three step process. First, a simple mean of the temperatures occurring on a day is found for each

day in the data set. The daily mean temperatures are grouped by the day they occur during the year, referred to as day of year or DOY. Next, the average of the data points that fall on the same day is calculated to obtain a mean yearly temperature cycle. Finally, the mean yearly cycle is subtracted from each data year to obtain the anomalous temperature variation of the meteorological temperature observations. A linear regression is performed on the final results to determine long term anomalous temperature trends. The slope of the trend line approximates the change in temperature per year at each station.

Temperature time series can be modeled as superposition of two functions i.e., a straight line representing long-term temperature trend and a wave (periodic function) representing annual temperature cycle. Mathematically, the observed temperature as a function of time is modeled as

$$\mathbf{T}(t) = \mathbf{T}_{trend}(t) + \mathbf{T}_{cycle}(t) + \mathbf{e} \quad (16)$$

where e represents the modeling error.

The trend line, T_{trend} , is given by $T_{trend}(t) = T_{ref} + mt$ where T_{ref} is the average temperature of the reference year and m is the long-term rate of temperature change. Since all stations have observations for 2010, it is used as the reference year. Any year can be selected as reference year that enables a consistent comparison of model parameters.

The periodic function, T_{cycle} , is modeled using multiyear daily mean (MDM). This approach assumes an average annual cycle determined from mean daily temperature.

It is more general approach compared to sinusoidal model and is not limited to sine function. In case of MDM T_{cycle} , there is no algebraic expression but a function with ordered pairs where abscissa is the day of year and ordinate is the temperature. The ordinate is determined by calculating multiyear average temperature for the corresponding abscissa. The deviation of the average annual cycle provides the estimate of T_{trend} . The deviation is determined by calculating residual temperature by subtracting the annual cycle curve from each year's temperature data. The T_{trend} can be determined by fitting a linear function to the residual temperature time series. Note that average temperature of the reference year (2010) is added to the residuals temperature to raise the line and make it comparable with T_{trend} from sinusoidal method.

3.4 Spatial Behavior of Temperature Trends and Urban Heat Island Intensity

This section describes the method applied to map the Urban Heat Island Intensity in Las Vegas. For the purposes of this research, UHII is defined as the reduced difference between minimum and maximum diurnal temperature in a region caused by UHI effects influenced by urban characteristics. An example of UHII is shown in Figure 10. Areas experiencing stronger UHI effects have less variation in diurnal temperature behavior. Furthermore, areas influenced by UHI development have temperature behavior remains relatively unchanged in the morning while evening temperatures are warmer than areas experiencing less UHII. This behavior of UHI effect in an area can be used to map UHII in Las Vegas.

3.4.1 Urban Heat Island Intensity Image

This method approximates the intensity of UHI at each cell of a LST raster image. The process is based on UHI definition that a strong UHI presence would have higher nighttime temperatures than regions with weaker UHI formations while midday temperatures should remain similar. The following method defined in this section consists of four steps. The first step is to calculate average surface temperature at each weather station for each LST image. The average surface temperature is correlated with observed noon and midnight temperatures to obtain linear trend parameters. The trend parameters are then joined to station point location layer and interpolated over the Las Vegas valley using inverse distance interpolation. The parameter maps are applied to a LST raster image to produce approximate air temperatures for the Las Vegas area at midnight and noon. The difference of these images should produce UHI intensity image indicating estimate UHI strength and size for study area for the day the TIR image was captured.

Land surface temperature is influenced by the same source of energy as the temperature of near surface atmosphere, the sun. Also, thermal energy is transferred between these media through radiation, convection, and conduction. There should be some dependence between the temperatures because of these environment interactions. Thus, influence between land surface temperatures and the near surface temperature decreases as the distance between the point weather observation and the differential surface increases. A radial distance from the meteorological station is established to estimate the land surface area that has some substantial relation with the temperature data observations collected at the meteorological station. This buffer zone is referred to as a

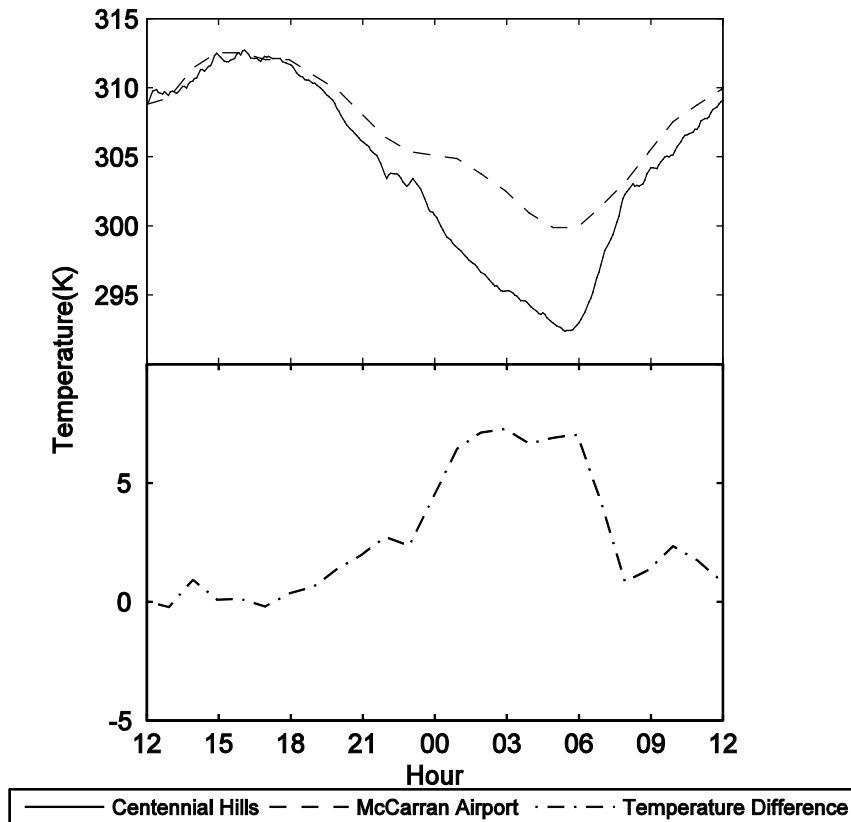


Figure 10: Diurnal comparison of weather stations experiencing different strengths of UHI.

region of interest, or ROI. These buffer zones are created from station location point data using the buffer tool in ArcMap. The mean LST is calculated within the ROI's for each remote sensed image captured by applying the zonal statistics tool.

When UHI is present it is assumed that the difference between the daily low and high temperature is lower than other areas. The difference between the midnight and noon image for a LST image indicates points that are prone to UHI effects wherever the raster cell difference is small. Thus, the mean difference of raster cells over undeveloped land can approximate the UHI boundary. Raster cell areas that fall below this mean would indicate areas where UHI are most likely to form.

3.5 Summary

Ground based temperature measurement and remote sensing data is used to study the temperature trends and spatial behavior. Temperature time series at ground stations is modeled using three methods to retrieve the slope of the temperature change. This change is related to the landcover characteristics.

Spatial maps of the urban heat island intensity are prepared based on the diurnal behavior of temperature. Ground based temperature (air) is related to remote sensing temperature (surface). This relationship is used to remote sensing land surface temperature to air temperature at noon and midnight. The difference of day and night temperature is used to map the urban heat island intensity. The spatial distribution of the urban heat island intensity is compared to landcover characteristics such as canopy cover, NDVI, and land climate zones.

CHAPTER 4: Temperature Trend Analysis at Weather Station Locations

This chapter provides the results produced by the temporal and spatial analysis approaches described in Chapter 3. The discussion of temporal and spatial analysis of trends in relation to landuse is also provided.

4.1 Low-pass Filter Analysis

The low-pass filter method produces no quantifiable numerical values allowing for direct comparison with other trend analysis methods, although it is also easier to estimate a long term temperature trend at most of the stations with the filtered data. Linear regression analysis was applied to the low-pass filter results to generate an approximate temperature change rates for comparison with other methods. The temperature trend results are listed in Table 3.

Table 3: Low-pass Filter Temperature Trends

No.	Station Name	m (K/yr)	b (K)	RMSE (K)
1	Henderson Executive Airport	-0.247	294.6	9.49
2	McCarran Airport	0.027	294.2	9.21
3	Nellis Air Force Base	-0.112	294.1	9.30
9	Legacy Golf Course Area	-0.023	295.4	9.14
10	Rhodes Ranch	0.278	290.9	8.76
11	Photo Patterns, East	-0.784	298.1	9.29
12	Neon Desert Weather, East Las Vegas	0.164	293.7	9.43
18	Palomino Estates	0.039	292.6	8.90
21	North Las Vegas Airport	0.014	293.5	9.05

Results show various rates of temperature change at different Las Vegas valley locations that range between -0.784 K/yr at station 11 to 0.278 K/yr at station 10.

The high root mean square error indicates any analysis of the results may not indicate the actual temperature behavior. The high error is due to using a regression method that is dissimilar to the temperature behavior. Other methods could be used to reduce the low-pass filter modeling error, although it would be more significant to apply the method to the original data instead of the low-pass filtered temperature data set.

4.2 Sinusoidal and MDM modeling analysis

Fourteen stations are selected that provide more than six years of observations. These stations are listed in Table 4 with the description of their landuse. The landuse is based on the integrated planned landuse map developed and shown in Figure 9.

Table 4: List of Ground Stations Showing Period of Temperature Data and Landuse

No	Station Name	Data Period	Landuse Zone
1	Henderson Executive Airport	2002 – 2012	Public Use
2	McCarran Airport	1948 – 2012	Public Use
3	Nellis AFB	1942 – 2012	Government
4	Seven Hills	2006 – 2011	Residential
5	MacDonald Ranch	2006 – 2011	Public Use
6	Sun City Anthem	2006 – 2011	Residential
7	Legacy Golf Course Area	2004 – 2011	Residential
8	Rhodes Ranch	2002 – 2011	Residential
9	Photo Patterns	2004 – 2011	Commercial
10	Neon Desert Weather, East Las Vegas	2004 – 2011	Public Use
11	NW Spring Valley	2005 – 2011	Residential
12	Photo Patterns	2005 – 2011	Residential
13	Palomino Estates	2001 – 2011	Residential
14	North Las Vegas Airport	1997 – 2012	Public Use

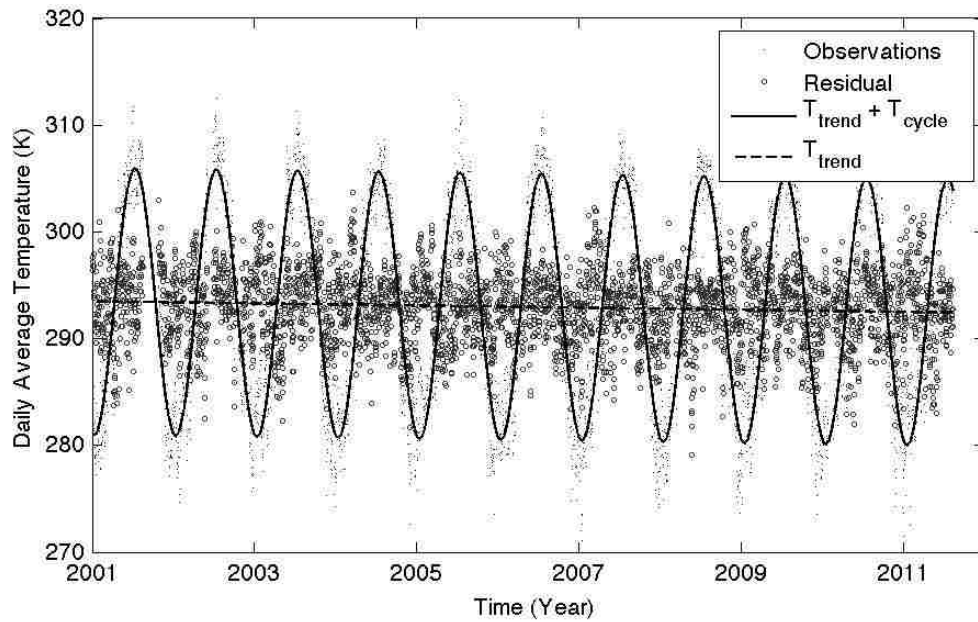


Figure 11: Plot showing time series of daily average temperature at Palomino Estates ground station with sinusoidal model fit and trend line.

4.3 Trend Analysis of Temperature

The temperature trend of Las Vegas has a spatially varying behavior. In order to study this, we analyze the trends during the 2000-2010 decade as the drought in the southwest US started around 2000. Some stations have shorter time series, but all stations cover 5 or more years. It is reasonable to assume that overall dataset would provide an acceptable estimate of the decadal trend. The sinusoidal and MDM trend approaches are applied to all stations for data since 2000. Figure 11 shows the sinusoidal model fit at station 13 whereas Figure 12 shows the MDM trend at the same station. The computed parameters are listed in Table 5.

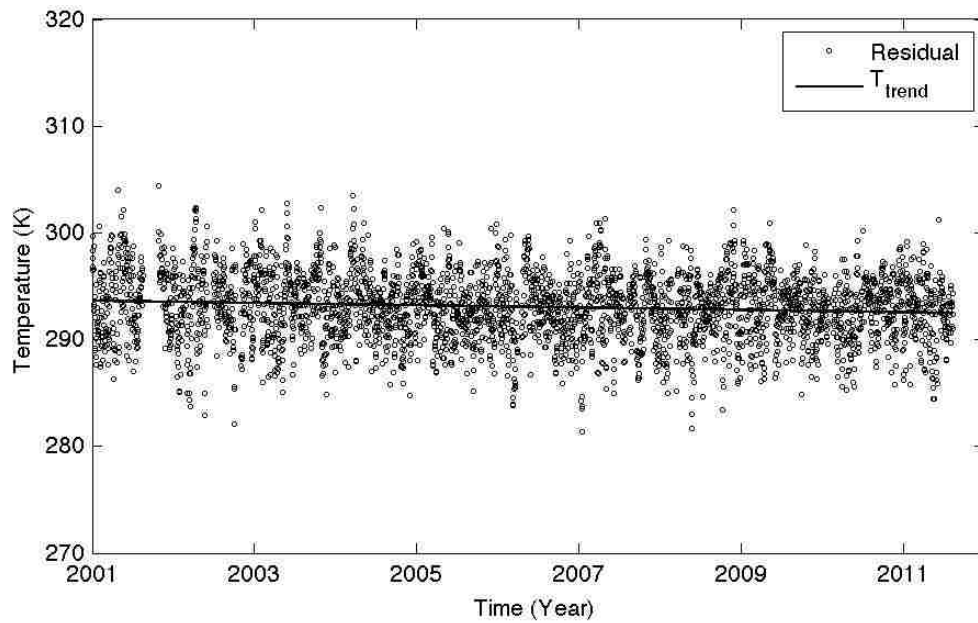
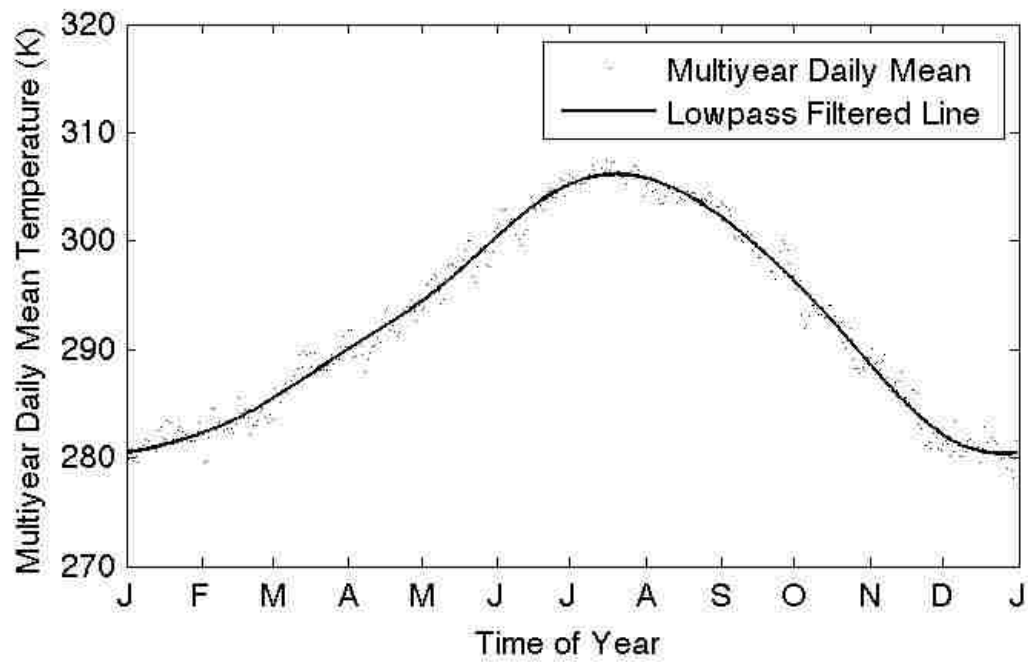


Figure 12: (top) Multiyear Daily Mean curve computed from all annual cycles and (bottom) Time series of the residual temperature.

Table 5: Model Parameters Using Sinusoidal and Residual Methods for All Ground Stations

Station No	Sinusoidal Method					MDM Method			Trend
	T_{ref} (K)	$365.25m$ (K/yr)	A (K)	T_{cycle} (day)	RMSE (K)	T_{ref} (K)	$365.25m$ (K/yr)	RMSE (K)	
1	293.14	-0.33	13.25	108	3.7	292.51	-0.319	3.35	High
2	294.32	-0.01	12.9	110	3.43	295.5	-0.016	3.24	Neg
3	293.66	-0.09	13.15	109	3.34	294.2	-0.095	3.14	Neg
4	293.13	-0.143	12.87	109	3.76	293.16	-0.178	3.31	Low
5	293.57	-0.279	13.38	110	5.31	293.69	-0.292	5.04	Med
6	292.57	-0.298	12.79	110	3.92	292.39	-0.332	3.5	Med
7	294.32	-0.025	13.08	107	3.17	294.28	-0.022	2.79	Neg
8	292.37	-0.017	12.28	111	3.53	292.44	-0.014	3.23	Neg
9	294.21	-0.1	12.89	107	3.34	294.06	-0.124	2.94	Low
10	293.97	0.006	13.01	107	3.23	294.02	-0.03	2.82	Neg
11	294.43	-0.084	12.06	107	3.3	293.15	-0.103	2.89	Low
12	292.18	0.09	12.28	109	3.42	292.42	0.076	3.07	Neg
13	292.59	-0.1	12.49	108	3.32	292.8	-0.108	3.13	Low
14	293.6	-0.119	12.77	109	3.39	293.31	-0.125	3.12	Low

The T_{ref} of both methods are comparable and generally lie in low 290s Kelvin range. Note that MDM T_{ref} values are calculated from observations and added to the residual temperature. The sinusoidal approach T_{ref} is within ± 1.3 K of MDM approach T_{ref} indicating that the model is a reasonable representation of the observations. Nevertheless, Root Mean Square Error (RMSE) of sinusoidal approach is relatively higher than MDM approach at all stations. This high modeling RMSE is due to the simplistic assumption of single sine wave T_{cycle} . This is also evident since the sinusoidal

model doesn't completely capture the peaks and valleys of the temperature data (See Figure 11). Overall, both approaches have most of the RMSE error values around 3.5 K and MDM method RSME error is about 10% less than sinusoidal approach. Note that sinusoidal method also lists the amplitude and phase. The amplitude shows the difference between maximum and minimum annual temperature. Sinusoidal model underestimates the amplitude by approximately 10K. The phase is the day of year when the sine wave crosses the average temperature line. This is consistent for all stations with an average value of 109th day.

The temperature trend is modeled by m parameter in both approaches. The parameter m is the rate of change of temperature in Kelvin per day (K/day). Since daily trend is a very small number, Table 5 reports yearly trend (K/yr) as $365.25m$. Negative and positive values mean decreasing and increasing temperature trends, respectively. Both approaches reveal negative numbers at most stations. In this analysis, the trend range is divided into 4 intensities, i.e., negligible (less than 0.1 K/yr), low (0.1 – 0.2 K/yr), medium (0.2 – 0.3 K/yr), and high (greater than 0.3 K/yr). Note that a 0.3 K/yr trend means 3 K temperature change per decade. The trend intensity of each station is listed in "Trend" column of Table 5 where downward arrow is shown to indicate decreasing trend. Clearly, there are no increasing trends during the last decade. Stations 1, 5, and 6 exhibit High or Medium trend while all remaining stations are Low or Negligible trend. These temperature trends are linked to changes in the urban landcover and landuse. Figure 13 compares these trends to change in the urban footprint between 2000 and 2010 using Landsat true color composite images. This figure shows the expansion of Las Vegas urban area. Although the city didn't expand much towards east

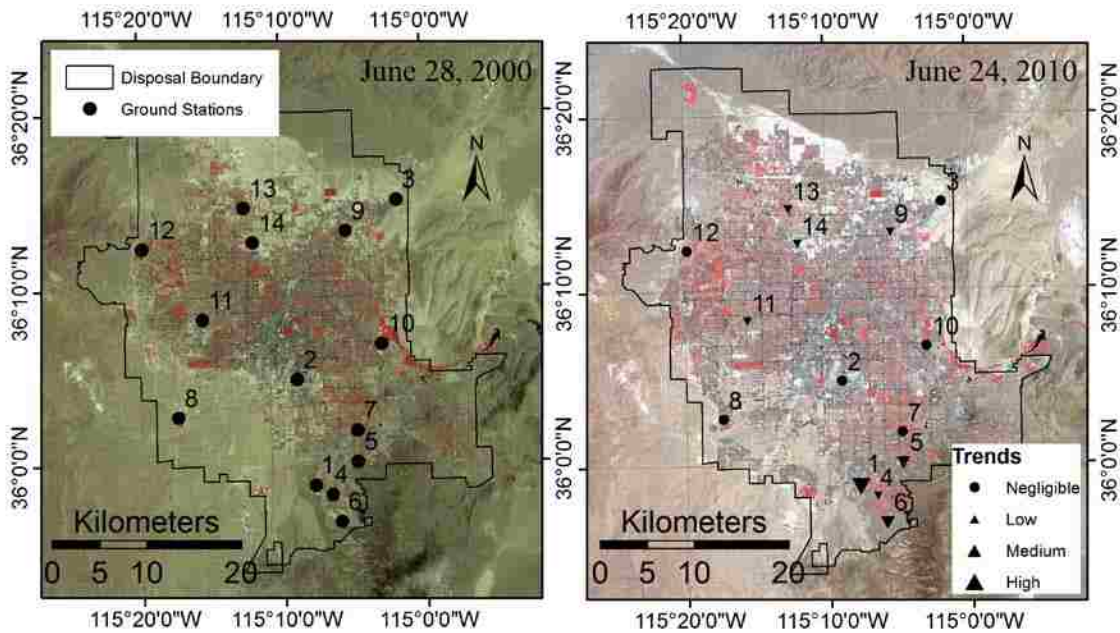


Figure 13: Las Vegas urban change between (left) 2000 and (right) 2010 as viewed by Landsat 5 Thematic Mapper.

due to the natural barrier from Frenchman mountain, the city has grown almost equally in all other three directions.

Figure 13 left panel image is overlaid with triangles showing magnitude of trend at ground stations. Although these are sparse points in a complex urban setting, two groups of trends are noted. The first group includes stations 9, 13, and 14 in the North Las Vegas with Low decreasing temperature trends and the second group includes stations 1, 4, 5, and 6 in the Southern Highlands with Low to High decreasing trends. Station 11 is located in the West and shows a Low decreasing trend. A comparison of left and right panel image pixels around of first and second groups reveals that these areas underwent development. Urban development in Las Vegas is accompanied with increased vegetation in the form of yards, trees, and parks. The decreasing temperature trends are reflective of the increased vegetation cover. This behavior has been also

observed by other investigators (Xian and Crane, 2006; Xian, 2008; Zang, 2011; Chow, 2012). The trends seen in North Las Vegas and Southern Highland are due to significant landuse transformation where many residential neighborhoods were developed during the last decade. Similar development happened in other areas such as Summerlin and Spring Valley but their temperature trends cannot be studied since these areas do not have measuring stations. Nevertheless, the available observations confirm that in an arid urban setting of Las Vegas, urban development results in decreasing temperature trends.

4.4 Trends Relation to NDVI Change

In order to relate the temperature trends to changes in vegetation, a comparison with NDVI change is analyzed. Figure 14 compares the annual average NDVI between 2000 and 2010 where darker pixels have higher green vegetation. At first glance the two images may look the same but a careful observation will reveal some subtle differences. For example, note that the spatial distribution of NDVI in Southern Highland and Summerlin in 2010 is darker than 2000. In order to emphasize such subtle changes, a difference image is calculated and shown in Figure 15. The points with temperature trends are overlaid to facilitate analysis. In the difference image, the darker areas represent increased NDVI values. Note that Southern Highland and Summerlin area show significant increase in NDVI during the last decade. In comparison to these areas, North Las Vegas has relatively lesser increase in NDVI. Thus, it is evident that despite urban development, the amount of vegetation is a key driving factor for temperature trends. The magnitude of temperature trends is proportional to the change in NDVI. Figure 16 plots the NDVI change against the magnitude of temperature trends. They are

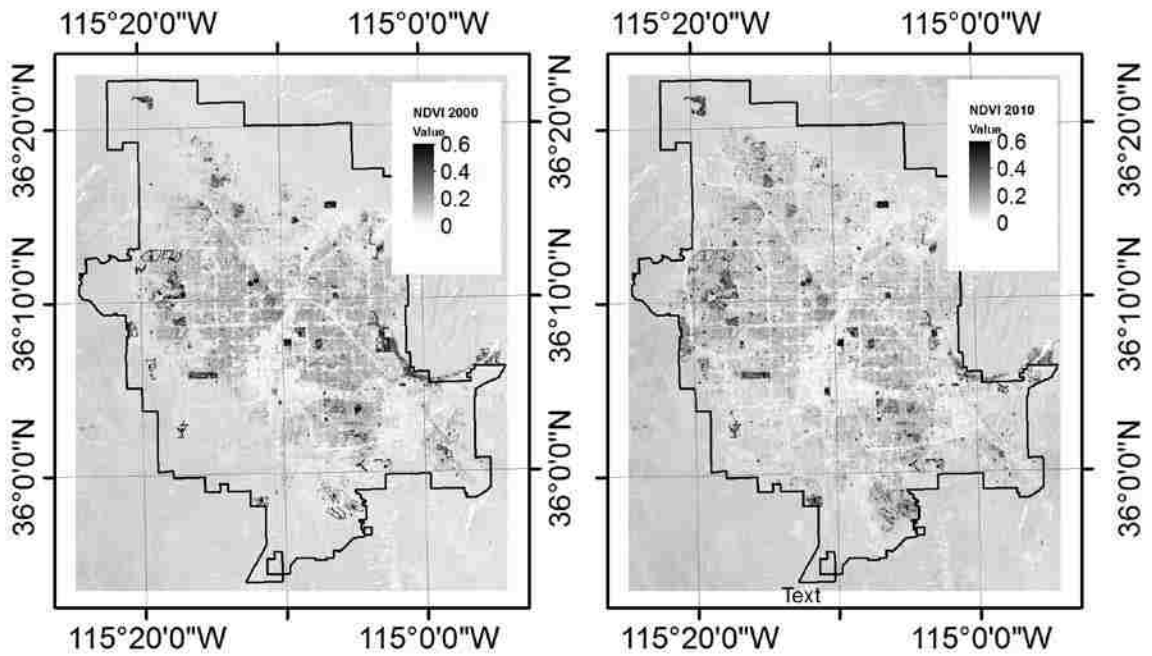


Figure 14: Spatial distribution of NDVI in the (left) 2000 and (right) 2010.

negatively correlated with $R=-0.655$. The p-value is 0.011 indicating a significant correlation. The regression fit is

$$\Delta_T = -0.78 - 36.8 \Delta_{ndvi}$$

where Δ_T is the change in temperature and Δ_{ndvi} is the change in NDVI. This analysis reveals that in an arid climate, an urban development accompanied by increased vegetation has a cooling effect.

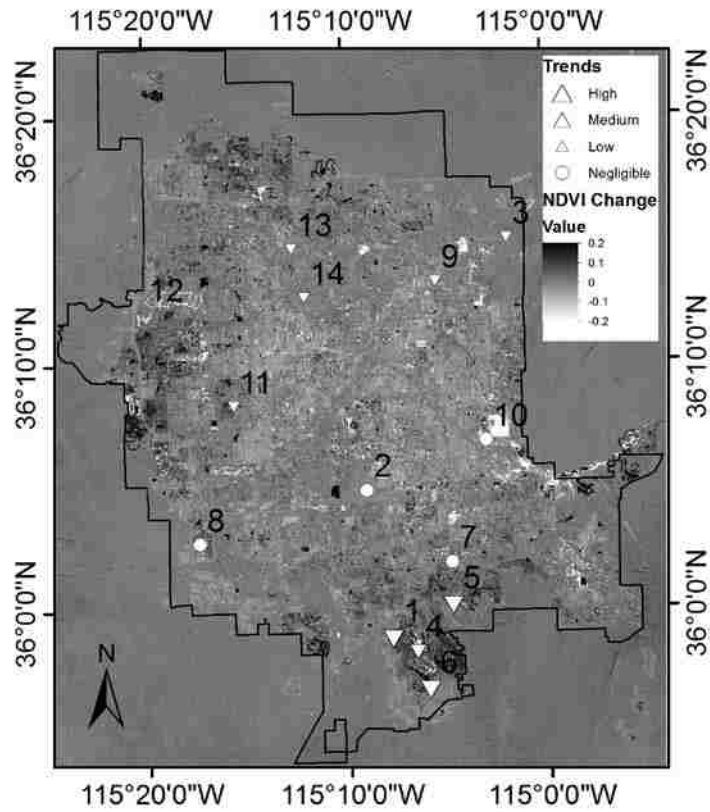


Figure 15: Spatial distribution of NDVI change between 2000 and 2010.

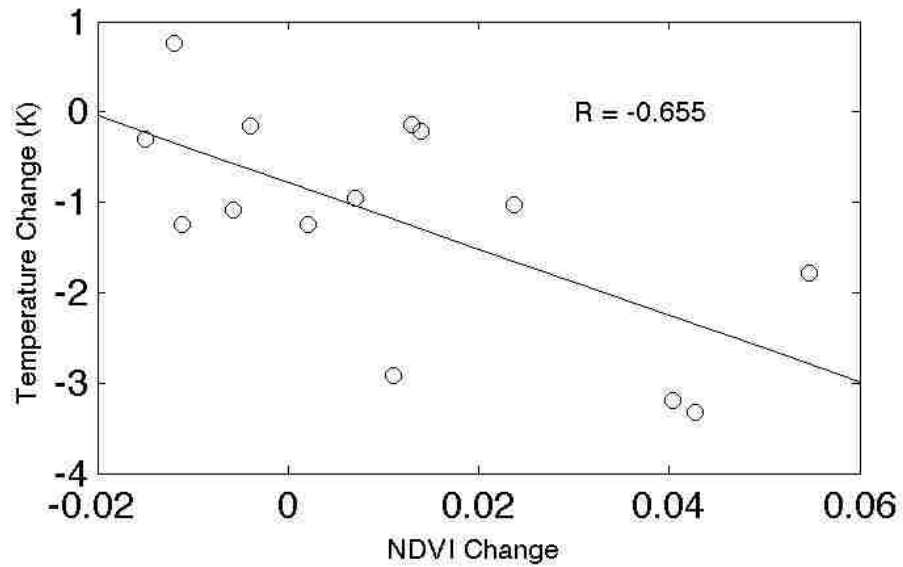


Figure 16: Plot of NDVI change vs. temperature change at all the ground stations between 2000 and 2010.

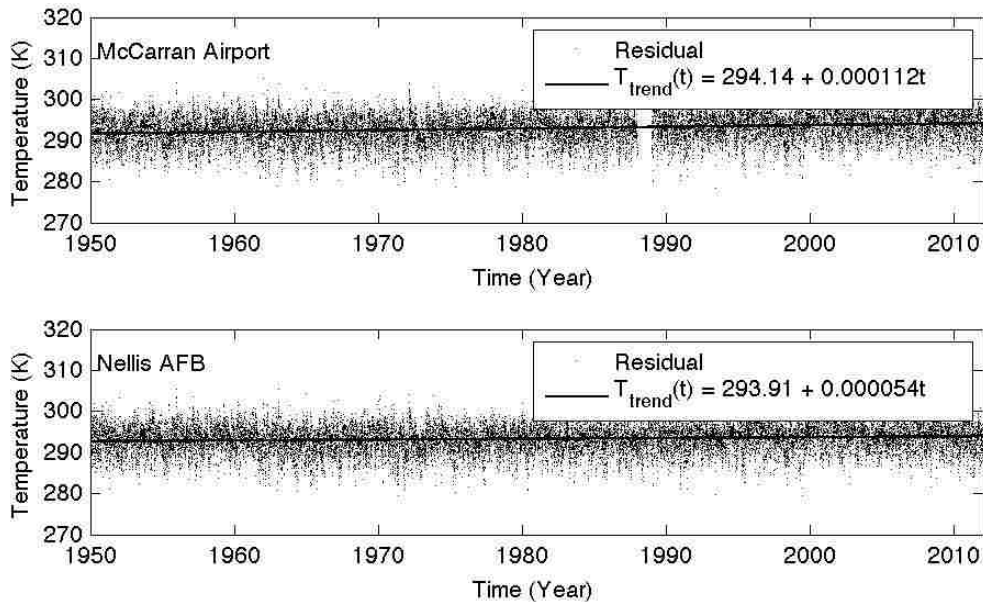


Figure 17: Long-term temperature trend using Multianual Daily Mean approach at (top) McCarran Airport and (bottom) Nellis Air Force Base.

4.5 Long term Temperature Trends

The following analysis is performed to understand the long term trends of temperature. Stations 2 (McCarran Airport) and 3 (Nellis Air Force Base) provide the longest temperature time series in Las Vegas. Figure 17 is a long term trend of the residual temperature using MDM approach discussed previously. The linear fit to this data shows that temperature trends at McCarran and Nellis are 0.04 K/yr and 0.02 K/yr. Based on the classification of 2000-2010 trends, these are less than 0.1 K/yr and thus negligible trends. But over the 6-decade period plotted in Figure 17, this trend reflects a 2.4 K and 1.2 K rise in temperature.

Figure 18 shows the same analysis of Figure 17 but excludes the final decade of temperature data at McCarran and Nellis. The long term trends decreased slightly to 0.034 K/yr and 0.017 K/yr respectively for McCarran and Nellis ground based weather

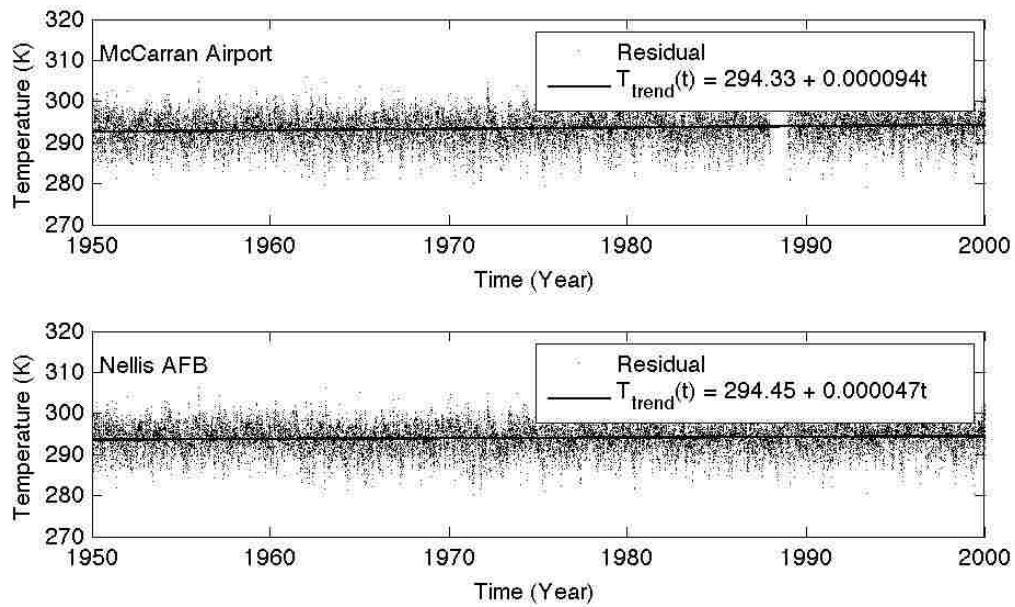


Figure 18: Long-term temperature trend excluding last decade using Multianual Daily Mean approach at (top) McCarran Airport and (bottom) Nellis Air Force Base.

stations. This translates to a 1.7 K and 0.8 K increase in temperature at these locations for the past 50 years. These results reflect a long term increasing temperature trend of the study area, which has been reversed during the last decade in the new developments of Las Vegas.

4.6 Summary

This chapter investigates the temperature trends in Las Vegas in relation to the vegetation change from urban development. Temperature trends are calculated from ground based measuring stations and vegetation change is determined using NDVI calculated from LandSat 5 Thematic Mapper imagery. Multiannual temperature observations are modeled as superposition of linear trend and annual cycle. In order to estimate temperature trend, the annual cycle is subtracted from the temperature observations. The annual cycle is modeled using two approaches i.e., sinusoidal model

and multiyear daily mean. MDM is a better representative of annual cycle with RMSE 10% less than sinusoidal model.

In general, the temperature shows a decreasing trend during 2000-2010. The stations with greater than 0.1 K/yr decrease correspond to North Las Vegas and Southern Highlands where annual average NDVI has increased during the last decade. As NDVI increase reflects increase in green vegetation, it is concluded that in an arid climate urban development with increased vegetation have a cooling effect. A significant correlation of 0.655 is observed between decadal change of NDVI and temperature in Las Vegas. Multi-decadal long term temperature trends are also analyzed at two ground stations with data from 1950 to 2000. These two stations are located at McCarran Airport and Nellis Air Force Base and show a gradual increase of 1.7 K/yr and 0.8 K/yr, respectively. Comparison of long term temperature trends with short term temperature trends supports the conclusion that urban modifications within the past decade have encouraged cooler temperatures in Las Vegas. More analysis would be required to define the relationship between short and long term temperature trends.

In 2008, City of Las Vegas adopted a resolution called “City of Las Vegas Urban Forestry Initiative” with goals of doubling Las Vegas tree canopy to 20% by 2035 (*City of Las Vegas*, 2008). There are many ongoing urban forestry efforts to increase the vegetation in Las Vegas. This research shows that vegetation cover has increased in many areas of Las Vegas. In arid climate, cooling of urban area with more vegetation comes at a cost of more water demand. Since Southwest US is undergoing a severe and historically longest drought, a careful analysis of benefit and cost of increased vegetation

must be conducted. This research provides an insight into the relationship between urban temperature and vegetation cover.

CHAPTER 5: Spatial Behavior of Temperature Trends and Urban Heat Island Intensity

This chapter provides urban heat island intensity results described in Chapter 3. The discussion of the spatial analysis in relation to landuse is also provided.

5.1 UHII from Regression Model of Wunderground and Landsat Temperature

This section describes the analysis performed to estimate temperature trends from the Landsat thermal remote sensing data and to create a map of urban heat island intensity. The process is started by defining the relationship between LST and ground based temperature observations. Wunderground temperature (WUT) is correlated with the average LST within a 500 meter radius of the ground base station location. A 500 meter radius was arbitrarily selected to represent the surface area that contributes heat energy to the air temperature at the station location. Figure 19 shows the time series of WUT and LST at weather station 11 located at a Photo Patterns store in North Las Vegas. Note that LST (red crosses) within a 500 meter radius of the weather station is, in general, higher than WUT (blue dots) as would be expected since WUT reflects the air temperature and LST is the surface temperature. The LST temporal resolution is coarse compared to WUT data but its spatial resolution is much finer compared to point based WUT data. Thus, we devised a technique to infer LST from the WUT.

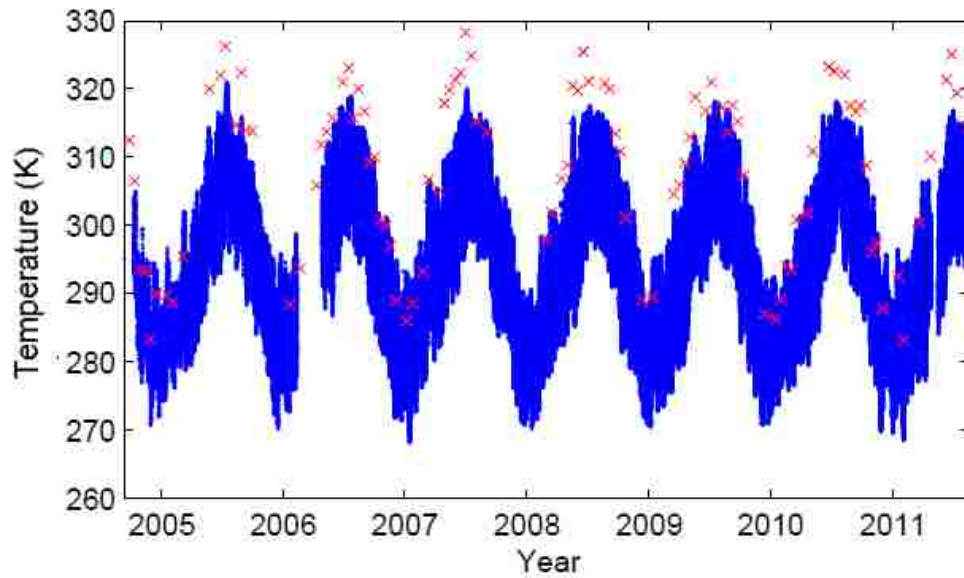


Figure 19: Graph showing a multi-year time series of air temperature observations and LST at station 11.

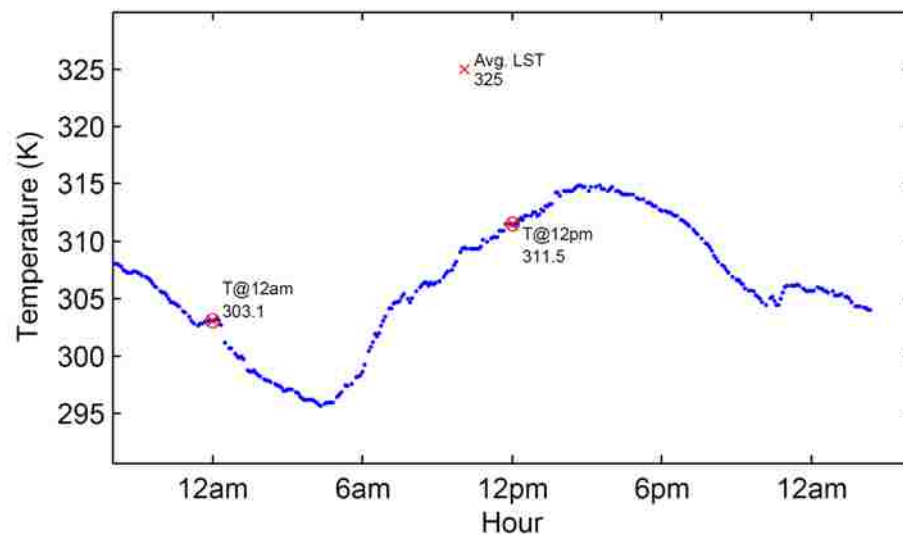


Figure 20: Graph showing typical diurnal variation of air temperature observations with LST from Landsat thermal imagery at 10AM at station 11.

This technique is based on developing a linear relationship between LST and air temperature values. As indicated earlier, the urban heat islands are areas where the night time temperature stays high due to the heat entrapment. Thus, it is hypothesized that the difference between the noon and midnight temperature at a given point is an indicator of its urban heat island intensity. Figure 20 shows the diurnal variation of the WUT data, which clearly shows the lowest point around sunrise and a peak in the afternoon.

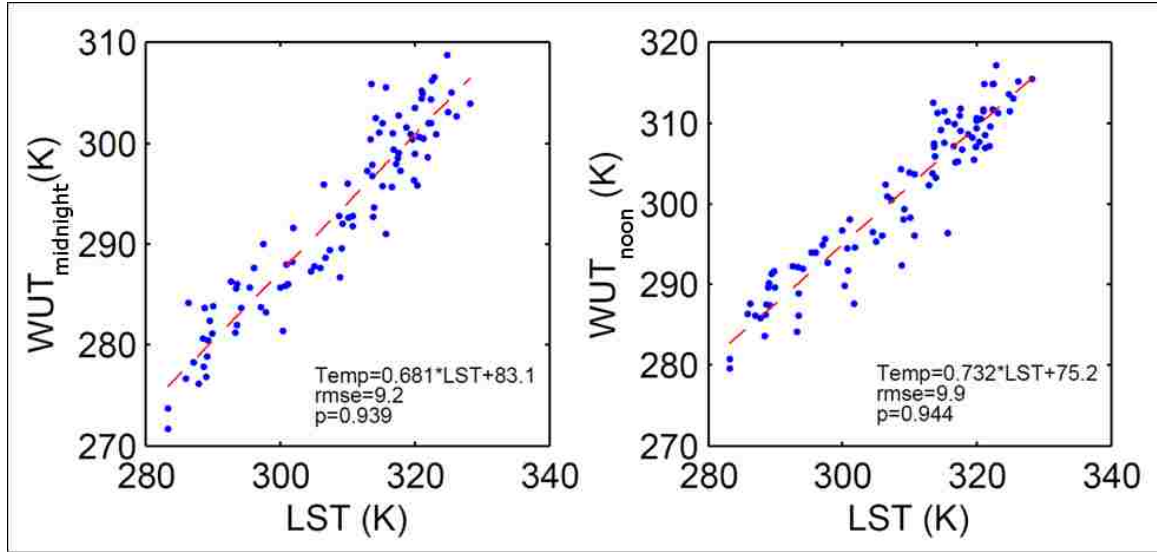


Figure 21: Graph showing relationships between average LST and (a) midnight air temperature and (b) noon air temperature at station 11.

A relationship was developed between LST and WUT at midnight ($WUT_{midnight}$) and at noon (WUT_{noon}) using the historical data at all WUnderground stations. The models are given by

$$WUT_{midnight} = A_m LST + B_m \quad (17)$$

$$WUT_{noon} = A_n LST + B_n \quad (18)$$

where A_m and B_m are parameters for midnight linear relationship and A_n and B_n are parameters for noon linear relationship. Figure 21 graphically demonstrates relationships at the Photo Patterns station. The model equations are also written in the figure. Model parameters are calculated for all the WUnderground stations and listed in Appendix C. Since these parameters reflect the relationship between WUT and LST, if available at each point these can be used to estimate WUT over the whole study area.

IDW interpolation was used to compute the model parameters everywhere in the region depicted in Figure 22. The images of the model parameters show spatial

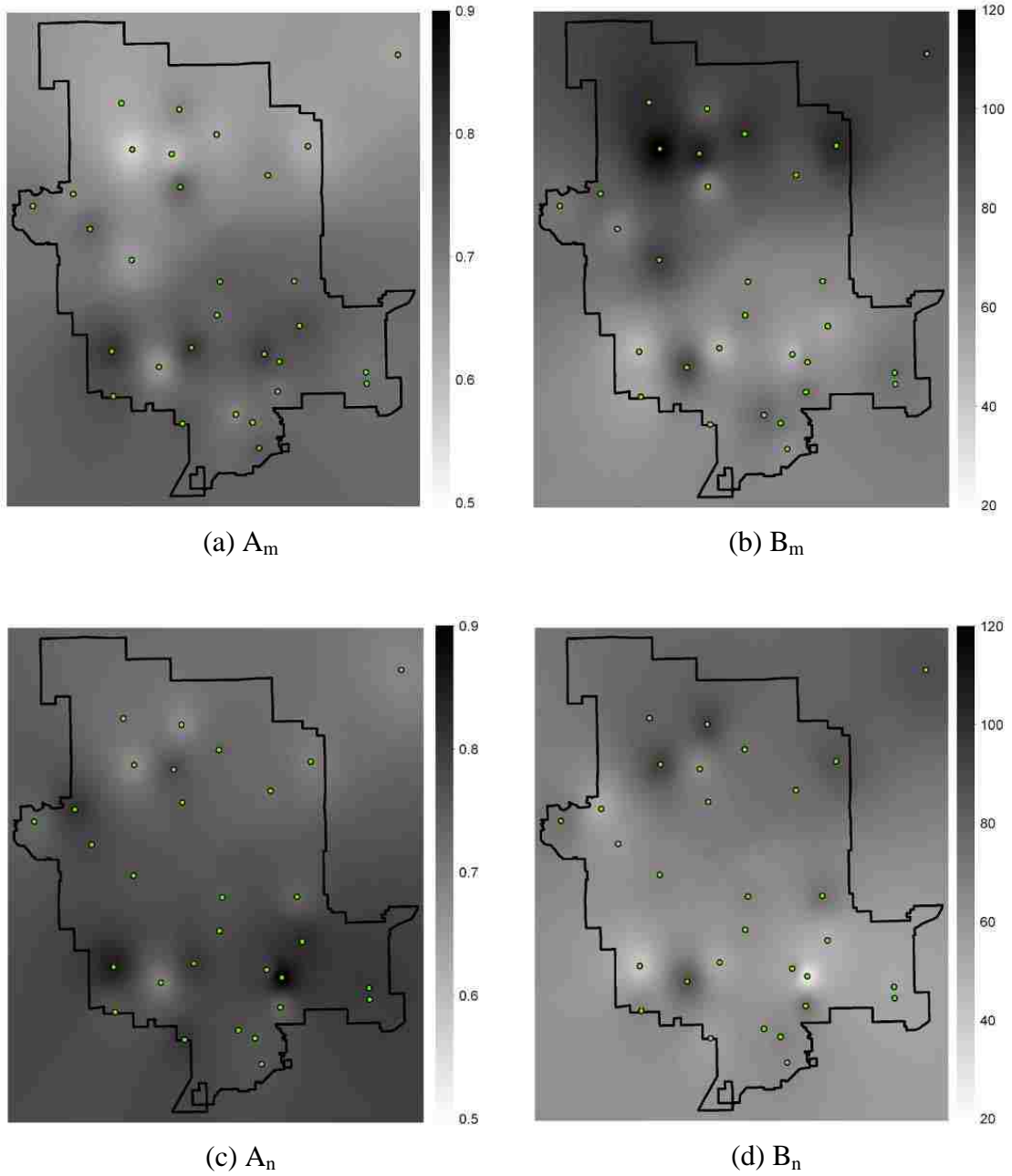


Figure 22: Images of linear model parameters for midnight [(a) and (b)], and noon [(c) and (d)].

coherence related to the urban thermal response. These images are used to compute the midnight and noon WUT values that reflect the spatial distribution of the air temperature.

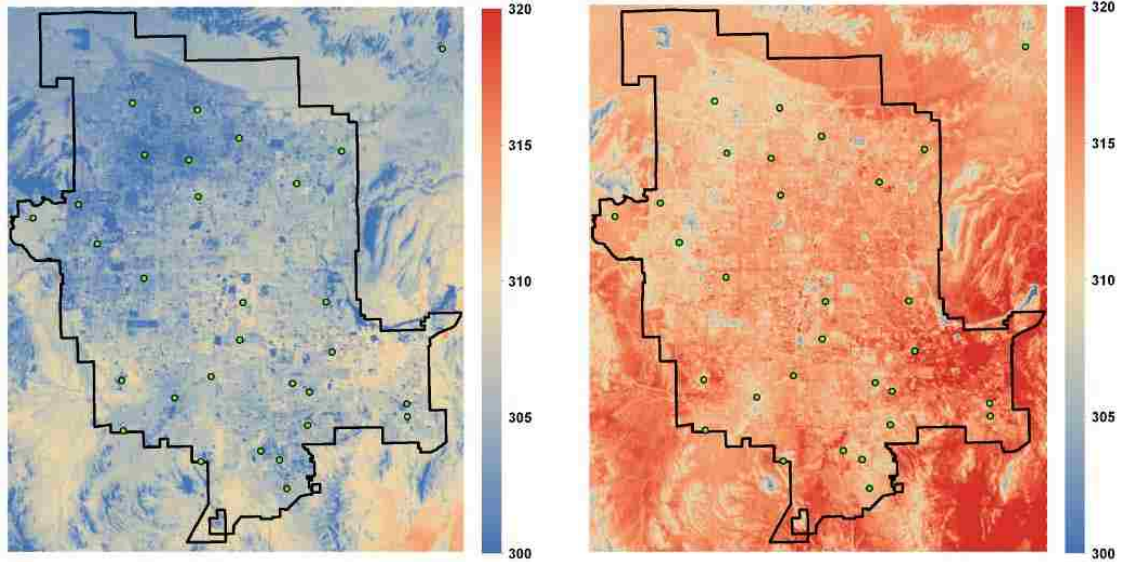


Figure 23: Images of estimated midnight (left) and noon (right) air temperature for June 27, 2011.

Using the Landsat thermal infrared image on June 27, 2011 WUT images of midnight and noon are calculated and shown in Figure 23. In general, the difference between night and day time temperature values is obvious showing relatively cooler night temperature. Moreover, these images also show the spatial variations that are dependent upon the urban layout as can be seen if compared to the Landsat optical image in Figure 6. As hypothesized earlier, the difference between noon and midnight air temperature is related to the urban heat island effect.

This method defines urban heat island intensity (UHII) as

$$UHII = WUT_{\text{midnight}} - WUT_{\text{noon}} \quad (4)$$

where higher values of UHII indicate an urban heat island.

Figure 24 shows the map of UHII computed from June 27, 2011 Landsat thermal imagery. Note that UHII is a negative number. $UHII = 0$ is the extreme case where the incoming energy is permanently trapped and midnight temperature is equal to the noon

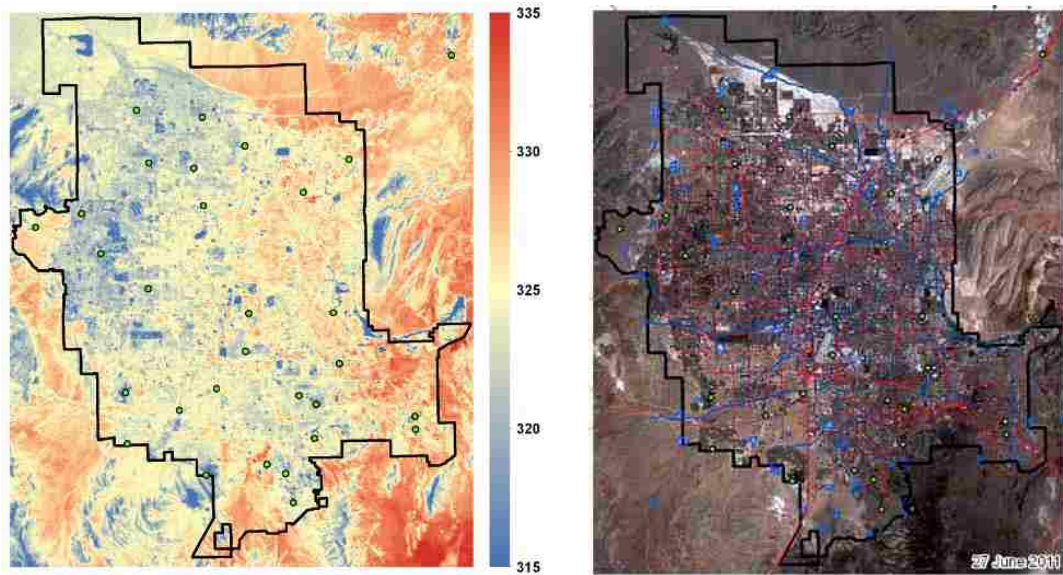
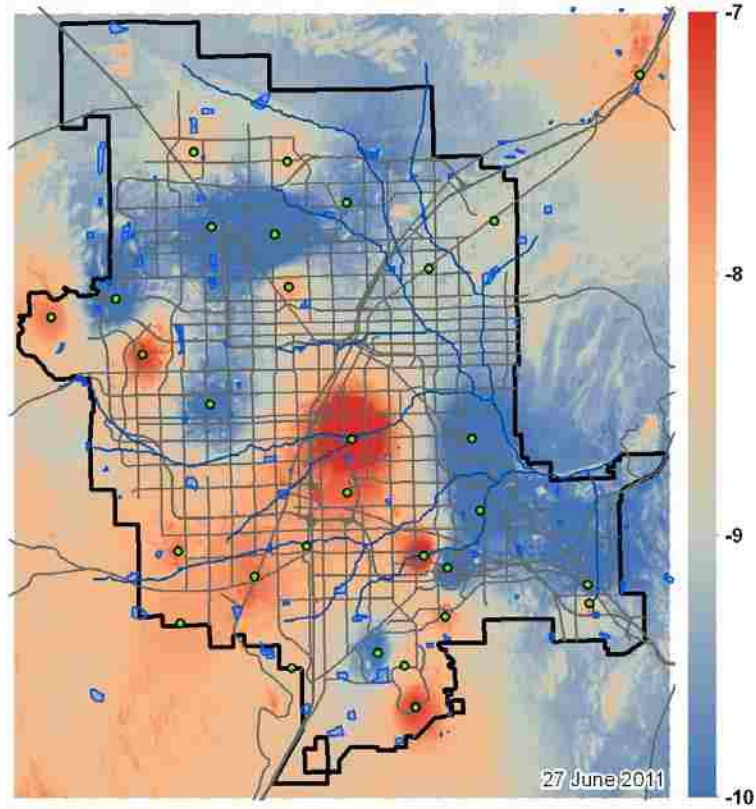


Figure 24: Urban Heat Island Intensity map of Las Vegas on June 27, 2011 (top), land surface temperature at 10:00 AM (bottom left), and Landsat 5 true color composite image (bottom right).

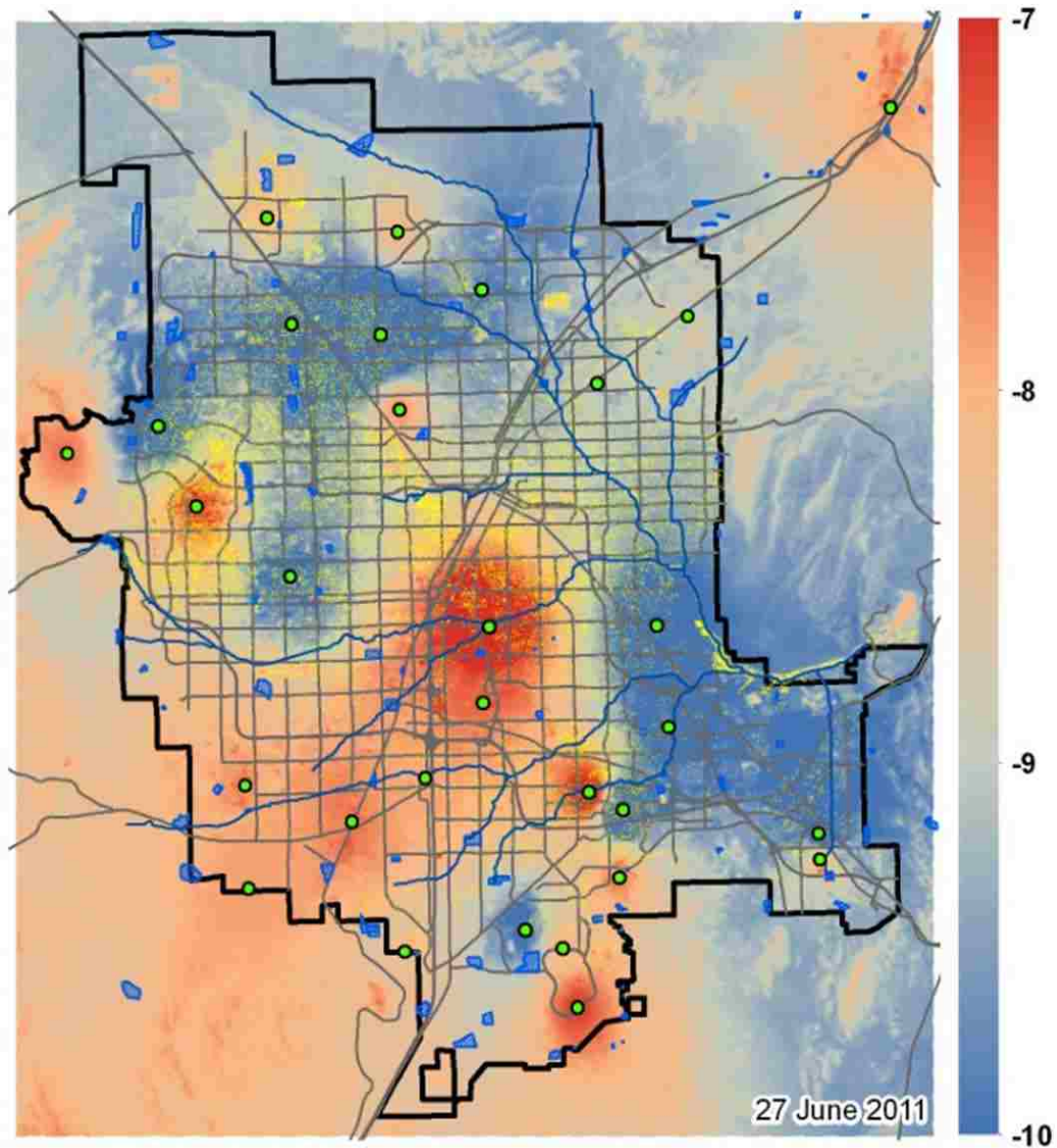


Figure 25: UHII map of Las Vegas on June 27, 2011 overlaid with SNWA 2006 tree canopy data.

temperature. As the UHII becomes negative (reduces), that indicates greater difference between midnight and noon temperature. It is seen that highest values of UHII = -5 are observed in several parts of the city. These areas mainly correspond to the airport, industrial areas, and older parts of the city. The newer developments, generally, have values less than -8.

In Figure 24, comparing UHII map with Landsat true color image reveals that urban regions with minimal temperature variation of UHII between -8.5 and -7 are located south of Tropicana Road and west of Green Valley Parkway / US Route 95. This area largely consists of undeveloped land with undetectable presence of landscape vegetation.

UHII values below -8.5 are mainly located in the City of Las Vegas and northeast City of Henderson districts. These regions correspond to dense residential developments with several dark green color swatches in the true color image that are usually associated with high water maintenance plants.

Figure 25 shows the UHII map with an overlay of the 2006 tree canopy cover data provided by the Southern Nevada Water Authority (Brandt, 2006). It is noted that UHII transitions from low to high as tree canopy density is reduced. Examples of this can be observed at the Aliante and North Las Vegas weather stations. The tree line also borders the southwest Las Vegas Valley region where low temperature variation is most likely to occur.

There are some areas that have dense tree canopies in the areas showing UHII greater than negative 8. Noticeable areas include the Angel Park NV US Las Vegas and Elkhorn Springs weather stations located in the northwest valley area. There is also dense vegetation located in the central study area around the Las Vegas US CEMP weather station. Low UHII values were expected to be found in these areas. A possible explanation for these contradictory occurrences is that the presence of dense foliage and trees in urban areas reduce the maximum daytime temperature in that region. Therefore,

less energy loss is required to attain rural nighttime temperatures which results in a high UHII value. Additional analysis should be considered to refine the process to distinguish between UHI and cool islands.

In order to further confirm the relation of UHII with tree canopy, we compare high resolution landuse information from NAIP imagery with computed UHII within 500m of selected stations. Figure 26 examines the UHII value increase between three residential communities. These areas are the locations of Sun City Anthem, Elkhorn Springs, and NW Spring Valley weather stations. UHII values in these increase from NW Spring Valley to Elkhorn Springs to Sun City Anthem. Examination of the true color composite images suggests NW Spring Valley has the highest vegetation density while Sun City Anthem has the least plant area. This confirms that UHII increases as plant coverage decreases. Figure 25 shows similar comparison over Weather Dog House and Arden NV US UPR meteorological stations with contrasting urban build-up. The Weather Dog House meteorological station is located in a dense residential region in the City of Las Vegas. The UHII map in this area shows that there is significant temperature cooling within this region. The Arden NV US UPR station is located in the southwest region of the study area where low urbanization has occurred and has high UHII. Comparison of the Weather Dog House and Arden NV US UPR stations shows that in the arid Las Vegas UHII decreases as land development increases.

Above examination of five selected stations indicates that Las Vegas areas where new urban development took place result in lower temperatures while in general, increased vegetation lower UHII. This implies that UHI are more likely to form in areas

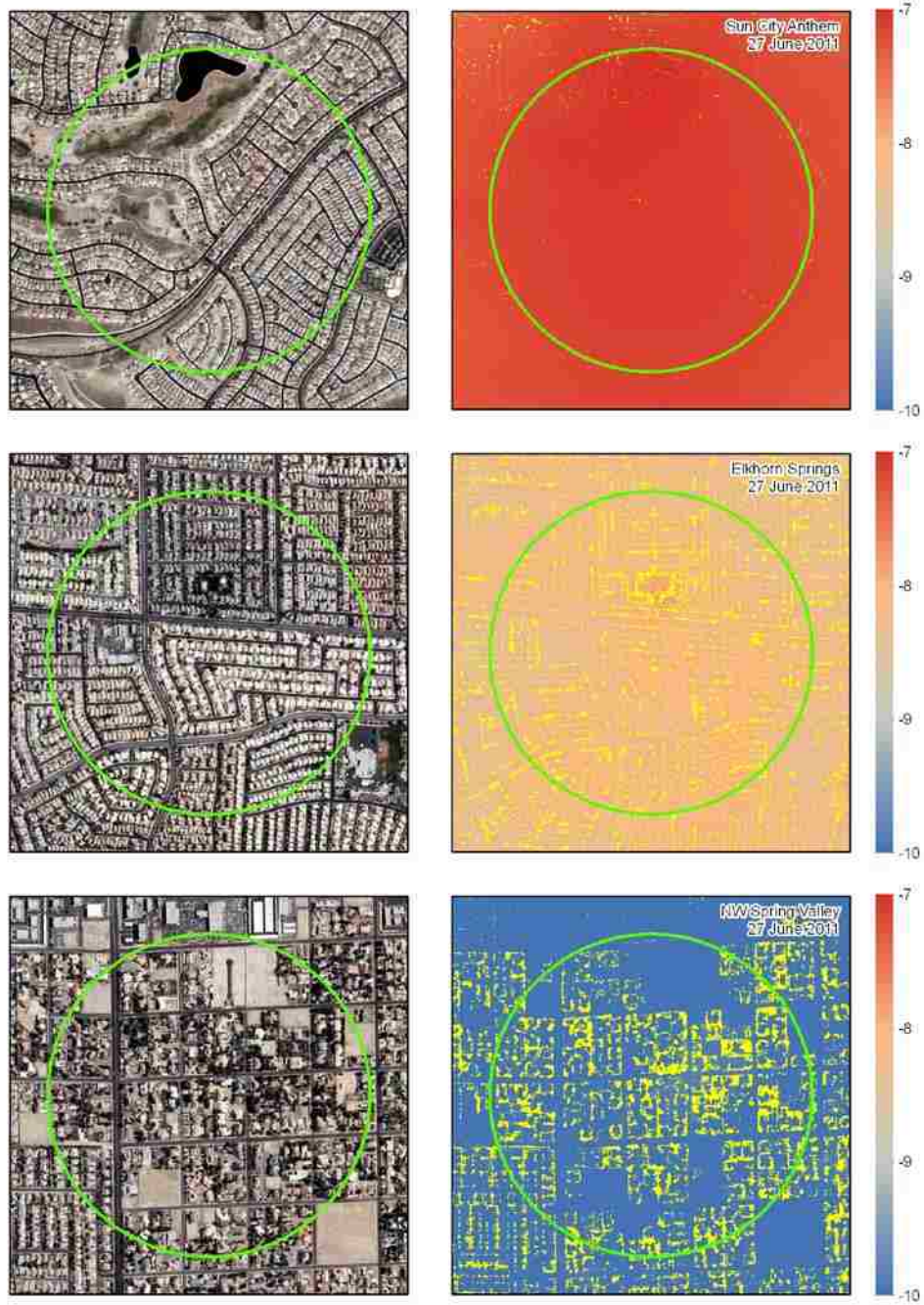


Figure 26: (Right) Urban Heat Island Intensity map of Las Vegas (Left) Landsat 5 true color composite image.

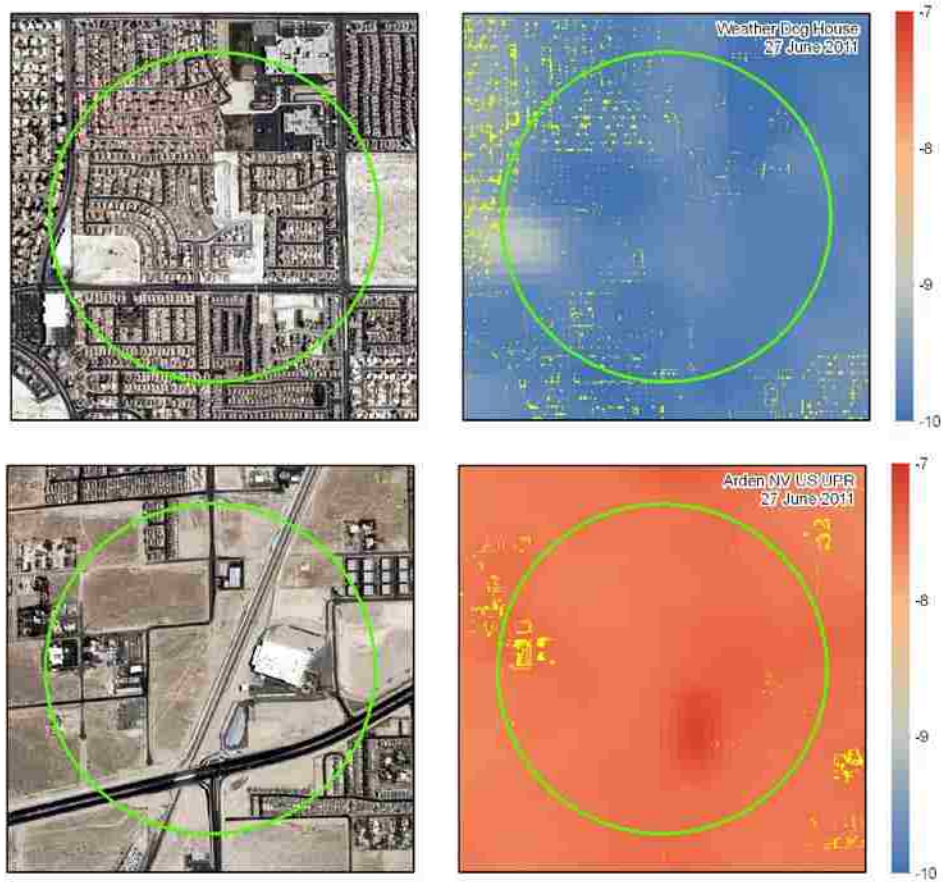


Figure 27: (Right) Urban Heat Island Intensity map of Las Vegas (Left) Landsat 5 true color composite image. with little or no vegetation whereas when new development takes place in an arid area it results in an overall cooling effect.

5.2 Las Vegas Valley Integrated Zone Map

The average value of trends and UHII were calculated for each landuse and the results are tabulated in following Table. Clearly, industrial and commercial areas have highest UHII with trends of -0.072 K/year and -0.066 K/year.

Table 6: Mean Change in Temperature by Zone Type

No.	Zone	Zone Code	Mean	
			UHII	Residual
1	Nellis AFB	AFB	-8.980	-0.028
2	Residential	B1	-8.962	-0.086
3	Commercial	B2	-8.529	-0.083
4	Industrial	B3	-8.644	-0.072
5	Public Use / Facilities	B4	-8.876	-0.066
6	Open Land	B5	-8.879	-0.124
7	ROW	B7	-9.120	-0.077
8	Unclassified	UZ	-8.537	-0.082

5.3 Temperature Trend Analysis of Landsat Thematic Mapper Temperature Data

The previous analysis was based on point measurements. In order to confirm these results and get a better spatial understanding of the trends, we also conducted trend analysis using Landsat Thematic Mapper derived temperature data. Similar procedure as described in Chapter 4 is used where mean annual response was subtracted to find residual temperature and slope of regression line was computed to estimate trend. This was performed for each pixel of Landsat TM image. Figure 28 shows the spatial map of the slope of residual temperature. This map illustrates that the old Las Vegas urban and rural area have continued to increase in surface temperature due to general climate trends, but the new development area in the fringe of the Las Vegas city does not show increasing trends. It is noted that in general the new development area has higher tree canopy cover.

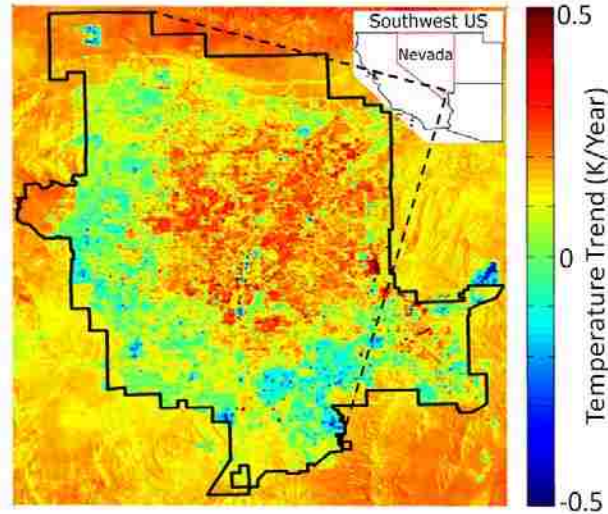


Figure 28: Spatial map of temperature trend estimated from Landsat TM 1990-2010 data.

It is noted that the analysis of Chapter 4 corresponds to air temperature whereas Figure 28 corresponds to the surface temperature. These two analyses provide different views of the urban heat island effect that surface level and canopy level.

5.4 Summary

The metropolis of Las Vegas has witnessed fast urban growth in the last few decades. This has resulted in modification of geophysical processes including the thermal response of the urban landscape resulting in urban heat island effect.

Urban heat island intensity (UHII) map is created by subtracting noon air temperature from the midnight air temperature. The images of midnight and noon temperature are created by developing relationships between the remote sensing and ground based temperature data. High UHII values indicate potential urban heat island and are observed at the airport and in the industrial areas. In order to measure the urban heat island effect, urban heat island intensity (UHII) is measured as a difference of

midnight and noon temperature. It is based on the observation that the urban heat islands that retain heat during the night do not cool down sufficiently and thus have temperatures closer to noon temperatures. Since midnight and noon temperature data of the whole valley is not available, it is estimated by developing regression relations between ground measurements and remote sensing thermal images. High UHII values indicate potential urban heat island and are observed at the airport and in the industrial areas. The results provide useful insight into the temporal thermal behavior of Las Vegas area.

CHAPTER 6: Summary, Conclusions, and Recommendations

Las Vegas has almost doubled its population during the last two decades and undergone exponential urban growth. The urban growth brings about changes that adversely impact the quality of urban life. This research investigated temperature trend in Las Vegas to understand its relation to landuse and urban heat island effect.

The results show that conversion of rural lands into urban developed areas has caused detectable changes to temperatures in Las Vegas. Improving open spaces in urban areas may assist in cooling nighttime temperatures in the city especially for developments that have included brush and trees in the landscape. The older parts of Las Vegas that existed before 1990, which also appears to be the densest urban area, experienced a slight temperature increase. This coincides with Xian's results showing Las Vegas urban surfaces with high NDVI being cool sinks except at places covered mainly with impervious surfaces (Xian et al., 2006; Xian, 2008).

Urban heat island effect is a serious problem in cities. Population growth and urban expansion in Las Vegas has induced fluctuations in temperature trends. Las Vegas, being in an arid region with limited water resources, faces challenges of balancing urban forestry with water consumption. Results presented in this thesis help to explain the temperature response to urban development in Las Vegas.

6.1 Conclusions

Studying the spatial and temporal trends of temperature observations and LST images in Las Vegas has revealed significant temperature behavior characteristics influenced by urban development. Las Vegas Valley experienced an average temperature

decrease of 0.15 K/yr for last 6 years. The largest cooling trend occurs in the southwest of City of Henderson at 0.32 K/yr. Long term temperature trend analysis at McCarran airport and Nellis air force ground weather stations show temperature trends switching from declining to increasing rates of change. This indicates that recent urban modifications cause air temperatures to change from a general warming trend of the study area to a local cooling trend. Analysis and comparison of rural station temperatures, or global climate data with long term temperature results is required to make a more conclusive statement.

Comparison of air temperatures with LST images exhibited a strong relationship that could be used to interpolate canopy temperatures for Las Vegas at different times of day. Correlation of noon and midnight canopy temperatures with LST produced correlation coefficients of 0.8 and 0.95. The noon and midnight canopy temperatures are related to LST linearly. The relationship between urban canopy temperatures and LST was used to calculate the difference between noon and midnight temperatures to estimate urban heat island intensity. The final map indicated that there is a strong UHI development in central Las Vegas north of McCarran Airport and developing UHI presence in the southwest Las Vegas region.

Comparison of the UHII map with NAIP imagery and the SNWA canopy at ground weather station locations show places with strong UHII that have minimal urban development and sparse vegetation. A direct comparison of change in LST between 1990 and 2010 shows that older parts of Las Vegas urban areas have warmer surface temperatures in 2010 while newer developments along the south and west edge of Las Vegas have noticeably cooler surfaces than 1990. Averaging the UHII values in areas

with similar Land Use characteristics show that Industrial and Commercial areas have slightly greater UHI effects than other landuses, although the difference is very minimal.

These conclusions contradict typical UHI behavior in climates with dense vegetation and rich with water resources. Urban expansion is expected to cause increased nighttime temperatures as percent impervious area increases and percent vegetation area decreases. Instead, the majority of north and south Las Vegas are experiencing decreasing temperature trends and few locations exhibited high UHII occurrence. It should be noted that the research results are site specific to Las Vegas and conclusions should only be compared to similar arid climates.

The basis of this research is to identify areas for green projects organized by the Nevada Division of Forestry within Las Vegas. The UHII map defines approximate locations where increased vegetation could be the most beneficial in reducing UHI effect. The easiest method for reducing the UHI is to increase the vegetation density which provides shade and moisture. This option can have the undesirable effect of increasing water consumption in a desert environment. Because water is a limited and precious resource in Nevada, it would be beneficial to understand the cost versus benefits of increasing water usage for maintaining vegetation to decrease nighttime temperatures.

6.2 Limitations

There were a few limitations identified in the methodology. The amount of long term ground weather station data available for this analysis is small since WUnderground has few stations that operated for longer than 5 years. Moreover, few stations were available in rural locations for comparison with urban results.

There are arbitrary values used in the analysis that can be adjusted to improve the final results. One parameter is the ROI area at a ground based weather station used to calculate the average LST for the WUT and LST correlation analysis. It is uncertain how much surface area contributes heat energy to the air at a ground weather station location. The other adjustable parameters are the midnight and noon temperatures used to define Urban Heat Island Intensity. It is unknown when the peak day temperature occurs and when at night UHI is the strongest. When these events occur during a given day is also influenced by the seasons and weather conditions. Sensitivity analysis will refine the research results. Analysis would also provide useful information about surface interaction with the atmosphere and UHI behavior.

Overlaying the SNWA canopy data over the UHII map has shown that there are some issues with the methodology in developing a UHII map. There is a strong vegetation presence in some of the areas with high UHII value. This is contrary to current theories that dense vegetation presence in an area inhibits the UHI effect. It is theorized that these areas are possibly cool islands. The maximum urban canopy temperature during the day is lower than normal in areas experiencing a cool island. This will also cause the morning temperatures to approach evening temperatures which also

reduces the diurnal temperature variation of a region erroneously identifying a cool island as a UHI region.

6.3 Recommendations for Future UHI Analysis

It is recommended that UHII mapping method be improved to distinguish between UHI and cool islands. Material properties effect on UHI development cannot be properly understood without being able to identify if temperatures in an area are higher than normal in the evening for UHI or lower than normal in the morning for cool islands.













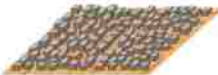




Sensitivity analysis of the ROI area and the reference times for UHII mapping should be performed to evaluate these parameters influence on the final results. Refined parameters would improve result analysis. Sensitivity analysis would also provide information about relationship characteristics of LST with air temperatures and investigate UHI peak occurrence at night.

This analysis applies several LST images that could be converted to UHII maps. A temporal analysis of these UHII maps would be useful in determining the evolution of UHI in Las Vegas. This could lead to useful analyses of historical UHI trends.

Little is done to compare actual surface properties on temperatures in Las Vegas. Observing diurnal temperature changes within, on, and above a surface made of different materials at a specific location can help evaluate the area and intensity of influence that several types of surfaces have on the immediate environment. This can lead to alternative methods to map UHI to directly verify thesis results.

An alternative method of mapping UHI development is to measure atmospheric temperature over a parcel that is being developed over a short period of time. Recording the temperature over neighboring land for a lengthy period of time. The UHI effect is theorized to induce an instantaneous change to the climate. Observing the temperature characteristics over land before, during, and after a property are developed can provide insights into UHI development especially if the analysis is able to include the growth of an entire community. This research provides useful insight into the temporal thermal behavior of the Las Vegas area.

APPENDIX B: Definition of Local Climate Zones (Stewart and Oke, 2012)

Built types	Definition	Land cover types	Definition
 <p>1. Compact high-rise</p>	Dense mix of tall buildings to tens of stories. Few or no trees. Land cover mostly paved. Concrete, steel, stone, and glass construction materials.	 <p>A. Dense trees</p>	Heavily wooded landscape of deciduous and/or evergreen trees. Land cover mostly pervious (low plants). Zone function is natural forest, tree cultivation, or urban park.
 <p>2. Compact midrise</p>	Dense mix of midrise buildings (3–9 stories). Few or no trees. Land cover mostly paved. Stone, brick, tile, and concrete construction materials.	 <p>B. Scattered trees</p>	Lightly wooded landscape of deciduous and/or evergreen trees. Land cover mostly pervious (low plants). Zone function is natural forest, tree cultivation, or urban park.
 <p>3. Compact low-rise</p>	Dense mix of low-rise buildings (1–3 stories). Few or no trees. Land cover mostly paved. Stone, brick, tile, and concrete construction materials.	 <p>C. Bush, scrub</p>	Open arrangement of bushes, shrubs, and short, woody trees. Land cover mostly pervious (bare soil or sand). Zone function is natural scrubland or agriculture.
 <p>4. Open high-rise</p>	Open arrangement of tall buildings to tens of stories. Abundance of pervious land cover (low plants, scattered trees). Concrete, steel, stone, and glass construction materials.	 <p>D. Low plants</p>	Featureless landscape of grass or herbaceous plants/crops. Few or no trees. Zone function is natural grassland, agriculture, or urban park.
 <p>5. Open midrise</p>	Open arrangement of midrise buildings (3–9 stories). Abundance of pervious land cover (low plants, scattered trees). Concrete, steel, stone, and glass construction materials.	 <p>E. Bare rock or paved</p>	Featureless landscape of rock or paved cover. Few or no trees or plants. Zone function is natural desert (rock) or urban transportation.
 <p>6. Open low-rise</p>	Open arrangement of low-rise buildings (1–3 stories). Abundance of pervious land cover (low plants, scattered trees). Wood, brick, stone, tile, and concrete construction materials.	 <p>F. Bare soil or sand</p>	Featureless landscape of soil or sand cover. Few or no trees or plants. Zone function is natural desert or agriculture.
 <p>7. Lightweight low-rise</p>	Dense mix of single-story buildings. Few or no trees. Land cover mostly hard-packed. Lightweight construction materials (e.g., wood, thatch, corrugated metal).	 <p>G. Water</p>	Large, open water bodies such as seas and lakes, or small bodies such as rivers, reservoirs, and lagoons.
 <p>8. Large low-rise</p>	Open arrangement of large low-rise buildings (1–3 stories). Few or no trees. Land cover mostly paved. Steel, concrete, metal, and stone construction materials.	VARIABLE LAND COVER PROPERTIES	
 <p>9. Sparsely built</p>	Sparse arrangement of small or medium-sized buildings in a natural setting. Abundance of pervious land cover (low plants, scattered trees).	Variable or ephemeral land cover properties that change significantly with synoptic weather patterns, agricultural practices, and/or seasonal cycles.	
 <p>10. Heavy industry</p>	Low-rise and midrise industrial structures (towers, tanks, stacks). Few or no trees. Land cover mostly paved or hard-packed. Metal, steel, and concrete construction materials.	<p><i>b. bare trees</i></p> <p><i>s. snow cover</i></p> <p><i>d. dry ground</i></p> <p><i>w. wet ground</i></p>	<p>Leafless deciduous trees (e.g., winter). Increased sky view factor. Reduced albedo.</p> <p>Snow cover >10 cm in depth. Low admittance. High albedo.</p> <p>Parched soil. Low admittance. Large Bowen ratio. Increased albedo.</p> <p>Waterlogged soil. High admittance. Small Bowen ratio. Reduced albedo.</p>

APPENDIX C: Parameters of the Midnight and Noon Air Temperature Models

Midnight Air Temperature Model Regression and Correlation Parameters

No	Station Name	StationID	Slope (m)	Intercept (b)	Correlation	RMSE	p-Value
1	Henderson Exec. Airport	KHND	0.688	79.9	0.827	6.694	0
2	McCarran Airport	KLAS	0.736	68.5	0.848	6.309	0
3	Nellis AFB	KLSV	0.620	103.2	0.771	6.366	0
4	Seven Hills	KNVHENDE12	0.720	72.0	0.881	9.233	0
5	MacDonald Ranch	KNVHENDE15	0.712	73.4	0.926	9.427	0
6	Bailes Home Weather	KNVHENDE16	0.709	75.5	0.822	10.094	0
7	Sun City Anthem	KNVHENDE17	0.751	62.1	0.939	9.380	0
8	Whitney Ranch	KNVHENDE22	0.778	53.4	0.961	9.815	0
9	Legacy Golf Course Area	KNVHENDE6	0.760	61.5	0.946	8.922	0
10	Rhodes Ranch	KNVLASVE11	0.812	45.4	0.932	8.961	0
11	Photo Patterns	KNVLASVE23	0.681	83.1	0.939	9.217	0
12	Neon Desert Weather	KNVLASVE25	0.734	65.5	0.930	9.809	0
13	NW Spring Valley	KNVLASVE32	0.649	94.2	0.937	7.920	0
14	Photo Patterns	KNVLASVE35	0.684	82.2	0.918	8.370	0
15	Centennial Hills	KNVLASVE54	0.560	120.0	0.861	7.939	0
16	Southern Highlands	KNVLASVE57	0.758	63.3	0.964	9.974	0
17	Elkhorn Springs	KNVLASVE8	0.624	101.4	0.915	8.552	0
18	Palomino Estates	KNVNORTH1	0.595	108.7	0.864	8.342	0
19	Weather Dog House	KNVNORTH6	0.628	99.6	0.889	8.772	0
20	Aliante	KNVNORTH8	0.683	82.7	0.896	9.275	0
21	North Las Vegas Airport	KVGT	0.742	65.4	0.841	6.351	0
22	Angel Park	MAPWN2	0.738	67.2	0.930	8.638	0
23	Henderson NV US	MC7282	0.804	46.1	0.931	8.581	0.000001
24	Henderson NV US CEMP	MCMP10	0.718	71.8	0.928	9.585	0
25	Las Vegas NV US CEMP	MCMP12	0.745	65.5	0.938	9.386	0
26	Las Vegas NV US CEMP	MD5026	0.775	53.6	0.927	9.907	0
27	Las Vegas NV US	MD5799	0.801	46.5	0.955	10.731	0
28	Summerlin West	MSMWN2	0.718	71.8	0.884	10.051	0.000001
29	Apex NV US UPR	MUP052	0.641	94.5	0.929	8.871	0
30	Arden NV US UPR	MUP076	0.656	91.1	0.948	8.122	0

Noon Air Temperature Model Regression and Correlation Parameters

No	Station Name	StationID	Slope (A_n)	Intercept (B_n)	Correlation	RMSE	p-Value
1	Henderson Exec. Airport	KHND	0.772	62.9	0.938	10.0	0
2	McCarran Airport	KLAS	0.777	62.6	0.943	9.9	0
3	Nellis AFB	KLSV	0.699	86.2	0.919	9.7	0
4	Seven Hills	KNVHENDE12	0.758	67.9	0.906	9.5	0
5	MacDonald Ranch	KNVHENDE15	0.734	73.8	0.938	9.4	0
6	Bailes Home Weather	KNVHENDE16	0.816	51.8	0.861	11.1	0
7	Sun City Anthem	KNVHENDE17	0.765	64.9	0.938	9.6	0
8	Whitney Ranch	KNVHENDE22	0.826	48.5	0.948	11.1	0
9	Legacy Golf Course Area	KNVHENDE6	0.910	24.4	0.959	10.5	0
10	Rhodes Ranch	KNVLASVE11	0.852	40.1	0.946	9.3	0
11	Photo Patterns	KNVLASVE23	0.732	75.2	0.944	9.9	0
12	Neon Desert Weather	KNVLASVE25	0.740	74.1	0.939	9.8	0
13	NW Spring Valley	KNVLASVE32	0.768	66.1	0.842	10.7	0
14	Photo Patterns	KNVLASVE35	0.815	50.6	0.954	9.5	0
15	Centennial Hills	KNVLASVE54	0.675	93.4	0.922	8.7	0
16	Southern Highlands	KNVLASVE57	0.808	55.7	0.949	10.8	0
17	Elkhorn Springs	KNVLASVE8	0.714	80.6	0.930	9.6	0
18	Palomino Estates	KNVNORTH1	0.775	63.7	0.946	9.9	0
19	Weather Dog House	KNVNORTH6	0.737	74.1	0.943	9.7	0
20	Aliante	KNVNORTH8	0.677	92.7	0.923	9.0	0
21	North Las Vegas Airport	KVGT	0.756	68.7	0.944	9.9	0
22	Angel Park	MAPWN2	0.785	59.5	0.908	10.1	0
23	Henderson NV US	MC7282	0.791	56.7	0.914	8.5	0
24	Henderson NV US CEMP	MCMP10	0.794	54.9	0.936	10.2	0
25	Las Vegas NV US CEMP	MCMP12	0.759	66.7	0.929	9.5	0
26	Las Vegas NV US CEMP	MD5026	0.760	66.5	0.917	9.8	0
27	Las Vegas NV US	MD5799	0.812	51.1	0.954	10.9	0
28	Summerlin West	MSMWN2	0.734	74.1	0.930	9.8	0
29	Apex NV US UPR	MUP052	0.685	88.0	0.941	9.5	0
30	Arden NV US UPR	MUP076	0.697	85.2	0.943	8.6	0

REFERENCES

- Ahani, H., Kherad, M., Kousari, M., Rezaeian-Zadeh, M., Karampour, M., Ejraee, F., & Kamali, S. (2012). An investigation of trends in precipitation volume for the last three decades in different regions of fars province, iran. *Theoretical and Applied Climatology*, 109(3-4), 361-382. doi:10.1007/s00704-011-0572-z
- Arnfield, A. J. (2003). Two decades of urban climate research: a review of turbulence, exchanges of energy and water, and the urban heat island. *International Journal of Climatology*, 23(1), 1-26.
- Bowers, S. A., & Hanks, R. J. (1962). Specific heat capacity of soils and minerals as determined with a radiation calorimeter. *Soil Science*, 94(6), 392-396.
- Brandt, J. (2006). *tree_canopy_06*. Unpublished manuscript.
- Brandt, J. (2008). Locating Turf and Water Features in the Las Vegas Valley, Nevada, Using Remote Sensing Techniques and GIS. ASPRS. Fall 2008 Pecora 17 Conference Proceedings.
<http://www.asprs.org/a/publications/proceedings/pecora17/0008.pdf>
- Building & fire safety. (2013). Retrieved February 15, 2013, from http://www.cityofhenderson.com/building_fire_safety/index.php
- Buyantuyev, A., & Wu, J. (2010). Urban heat islands and landscape heterogeneity: linking spatiotemporal variations in surface temperatures to land-cover and socioeconomic patterns. *Landscape Ecology*, 25(1), 17-33.

Chander, G., Markham, B. L., & Helder, D. L. (2009). Summary of current radiometric calibration coefficients for Landsat MSS, TM, ETM+, and EO-1 ALI sensors.

Remote sensing of environment, 113(5), 893-903.

Chen, X. L., Zhao, H. M., Li, P. X., & Yin, Z. Y. (2006). Remote sensing image-based analysis of the relationship between urban heat island and land use/cover

changes. *Remote sensing of environment*, 104(2), 133-146.

Comprehensive planning demographics. Retrieved from

http://www.clarkcountynv.gov/depts/comprehensive_planning/demographics/documents/historicalcclvaveragepopgrowthrate.xls

Converting landsat TM and ETM+ thermal bands to temperature. (2010). Unpublished manuscript. Retrieved 13Aug2012.

Emmanuel, R., & Kruger, E. (2012). Urban heat island and its impact on climate change resilience in a shrinking city: The case of glasgow, UK. *Building and Environment*, 53, 137-149. doi:10.1016/j.buildenv.2012.01.020

Frumkin, H. (2002). Urban sprawl and public health. *Public health reports*, 117(3), 201.

Geller, T. (2007). Envisioning the wind: Meteorology graphics at weather underground.

IEEE Computer Graphics and Applications, 27(5), 92-97.

doi:10.1109/MCG.2007.124

Geographic information services (GIS). (2013). Retrieved February 15, 2013, from

<http://www.cityofhenderson.com/gis/index.php>

Geographic information system management office. Retrieved Sept. 7, 2012, from
<http://www.clarkcountynv.gov/depts/ccgis/pages/default.aspx>

Howard, L. (2011). *Climate of london* International Association for Urban Climate.

Kato, S., & Yamaguchi, Y. (2005). Analysis of urban heat-island effect using ASTER and ETM+ Data: Separation of anthropogenic heat discharge and natural heat radiation from sensible heat flux. *Remote Sensing of Environment*, 99(1), 44-54.

Keller-McNulty, S., & Kennedy, W. J. (1987). Error-free computation of the moore-penrose inverse with application to linear least squares analysis. *Journal of Statistical Computation and Simulation*, 27(1), 45-64.

doi:10.1080/00949658708810979

Laas, A., Nõges, P., Kõiv, T., & Nõges, T. (2012). High-frequency metabolism study in a large and shallow temperate lake reveals seasonal switching between net autotrophy and net heterotrophy. *Hydrobiologia*, 694(1), 57-74.

Landsat 7 science data users handbook (2008). In Landsat Project Science Office (Ed.), Greenbelt, Maryland: National Aeronautics and Space Administration.

Laory, I., Trinh, T. N., & Smith, I. F. C. (2011). Evaluating two model-free data interpretation methods for measurements that are influenced by temperature. *Advanced Engineering Informatics*, 25(3), 495-506. doi:10.1016/j.aei.2011.01.001

- Lo, C. P., Quattrochi, D. A., & Luvall, J. C. (1997). Application of high-resolution thermal infrared remote sensing and GIS to assess the urban heat island effect. *International Journal of Remote Sensing*, 18(2), 287-304.
- Lo, C. P., & Quattrochi, D. A. (2003). Land-use and land-cover change, urban heat island phenomenon, and health implications: a remote sensing approach. *Photogrammetric Engineering and Remote Sensing*, 69(9), 1053.
- Moran, M. J., Shapiro, H. N., Boettner, D. D., & Bailey, M. (2010). *Fundamentals of engineering thermodynamics*. Wiley. com.
- Oke, T. R. (1973). City size and the urban heat island. *Atmospheric Environment*, 7(8), 769-779. doi: 10.1016/0004-6981(73)90140-6
- Oke, T. R. (1978). *Boundary layer climates*. London: Methuen & Co Ltd.
- Oke, T. R. (1988). The urban energy balance. *Progress in Physical Geography*, 12(4), 471-508.
- Reducing urban heat islands: Compendium of strategies - urban heat island basics* (2008). In Climate Protection Partnership Division (Ed.), . Washington, DC: U.S. Environmental Protection Agency.
- Remar, Alex. (2010). Urban Heat Island Expansion in the Greater Las Vegas Metropolitan Area. *California Polytechnic State University*.
<http://digitalcommons.calpoly.edu/cgi/viewcontent.cgi?article=1008&context=erscs>
[p](#)

- Sherman, D. L., Patel, C. B., Zhang, N., Rossell, L. A., Tsai, Y. C., Thakor, N. V., & Mirski, M. A. (2004). Sinusoidal modeling of ictal activity along a thalamus-to-cortex seizure pathway I: New coherence approaches. *Annals of Biomedical Engineering*, 32(9), 1252-1264. doi:10.1114/B:ABME.0000039359.65273.9b
- Stewart, I. D., & Oke, T. R. (2012). Local climate zones for urban temperature studies. *Bulletin of the American Meteorological Society*, 93(12), 1879-1900.
- Stone, B., & Norman, J. M. (2006). Land use planning and surface heat island formation: A parcel-based radiation flux approach. *Atmospheric Environment*, 40(19), 3561-3573. doi:10.1016/j.atmosenv.2006.01.015
- Streutker, D. R. (2003). Satellite-measured growth of the urban heat island of Houston, Texas. *Remote Sensing of Environment*, 85(3), 282-289.
- Taha, H. (1997). Urban climates and heat islands: Albedo, evapotranspiration, and anthropogenic heat. *Energy and Buildings*, 25(2), 99-103. doi: 10.1016/S0378-7788(96)00999-1
- Tran, H., Uchihama, D., Ochi, S., & Yasuoka, Y. (2006). Assessment with satellite data of the urban heat island effects in Asian mega cities. *International Journal of Applied Earth Observation and Geoinformation*, 8(1), 34-48.
- USGS global visualization viewer. Retrieved Aug. 12, 2012, from <http://glovis.usgs.gov/index.shtml>
- Voogt, J. A., & Oke, T. R. (2003). Thermal remote sensing of urban climates. *Remote Sensing of Environment*, 86(3), 370-384. doi:10.1016/S0034-4257(03)00079-8

- Xian, G., & Crane, M. (2006). An analysis of urban thermal characteristics and associated land cover in tampa bay and lasvegas using landsat satellite data. *Remote Sensing of Environment*, 104(2), 147-156. doi:10.1016/j.rse.2005.09.023
- Xian, G. (2008). Satellite remotely-sensed land surface parameters and their climatic effects for three metropolitan regions. *Advances in Space Research*, 41(11), 1861-1869. doi:10.1016/j.asr.2007.11.004
- Weng, Q., Lu, D., & Schubring, J. (2004). Estimation of land surface temperature–vegetation abundance relationship for urban heat island studies. *Remote sensing of Environment*, 89(4), 467-483.
- Wundermap. Retrieved 08 February, 2013, from <http://www.wunderground.com/wundermap/>
- WunderWiki main page. Retrieved 08 February, 2013, from http://wiki.wunderground.com/index.php/Main_Page
- Yang, C., & Wei, G. (2009). Sinusoidal parameters estimation in speech sinusoidal model. Paper presented at the *2009 International Conference on Machine Learning and Cybernetics, July 12, 2009 - July 15, , 6* 3633-3638. doi:10.1109/ICMLC.2009.5212796
- Yuan, F., & Bauer, M. E. (2007). Comparison of impervious surface area and normalized difference vegetation index as indicators of surface urban heat island effects in

landsat imagery. *Remote Sensing of Environment*, 106(3), 375-386.

doi:10.1016/j.rse.2006.09.003

Zha, Y., Gao, J., Jiang, J., Lu, H., & Huang, J. (2012). Normalized difference haze index:

A new spectral index for monitoring urban air pollution. *International Journal of*

Remote Sensing, 33(1), 309-321. doi:10.1080/01431161.2011.59501

VITA

Graduate College
University of Nevada, Las Vegas

Adam Leland Black

Degrees:

Bachelor of Science, Civil and Environmental Engineering, 2009
University of Nevada, Las Vegas

Thesis Title:

Temperature Trends and Urban Heat Island Intensity Mapping of the Las Vegas
Area

Thesis Examination Committee:

Chairperson, Dr. Haroon Stephen, Ph. D
Committee Member, Dr. Sajjad Ahmad, Ph. D
Committee Member, Dr. Jacimaria Batista, Ph. D
Graduate Faculty Representative, Daniel Thompson, Ph. D